inorganics

MDPI

Review

The Redox Active [2Fe-2S] Clusters: Key-Components of a Plethora of Enzymatic Reactions—Part I: Archaea

Maddalena Corsini and Piero Zanello *

Department of Biotechnology, Chemistry and Pharmacy, University of Siena, Via Aldo Moro 2, 53100 Siena, Italy; maddalena.corsini@unisi.it

* Correspondence: piero.zanello@unisi.it

Abstract: The earliest forms of life (i.e., Archaea, Bacteria, and Eukarya) appeared on our planet about ten billion years after its formation. Although Archaea do not seem to possess the multiprotein machinery constituted by the NIF (Nitrogen Fixation), ISC (Iron Sulfur Cluster), SUF (sulfur mobilization) enzymes, typical of Bacteria and Eukarya, some of them are able to encode Fe-S proteins. Here we discussed the multiple enzymatic reactions triggered by the up-to-date structurally characterized members of the archaeal family that require the crucial presence of structurally characterized [2Fe-2S] assemblies, focusing on their biological functions and, when available, on their electrochemical behavior.

Keywords: Archaea; enzymatic reactions; [2Fe-2S] clusters; structure; electrochemistry

Citation: Corsini, M.; Zanello, P. The Redox Active [2Fe-2S] Clusters: Key-Components of a Plethora of Enzymatic Reactions—Part I: Archaea. *Inorganics* **2022**, *10*, 14. https://doi.org/10.3390/inorganics10010014

Academic Editor: Sandrine Ollagnier de Choudens

Received: 20 December 2021
Accepted: 4 January 2022
Published: 17 January 2022

1. Introduction

The Earth is 4.6 billion years old and microbial life is thought to have first appeared between 3.8 and 3.9 billion years ago; in fact, 80% of Earth's history was exclusively microbial life, which is still the dominant life form on Earth. It has been estimated that the total number of microbial cells on Earth is of the order of 2.5×10^{30} cells [1], which, considering the typical carbon content per cell, leads to about 550 gigatons of carbon (Gt C) of biomass distributed among all of the kingdoms of life. In particular, plants contribute about 450 Gt C (i.e., the dominant kingdom), animals about 2 Gt C, Bacteria about 70 Gt C, and Archaea about 7 Gt C [2].

In this connection, based on molecular phylogenetics, Woese created the well-known ribosomal "Tree of Life" [3–8] (Figure 1).

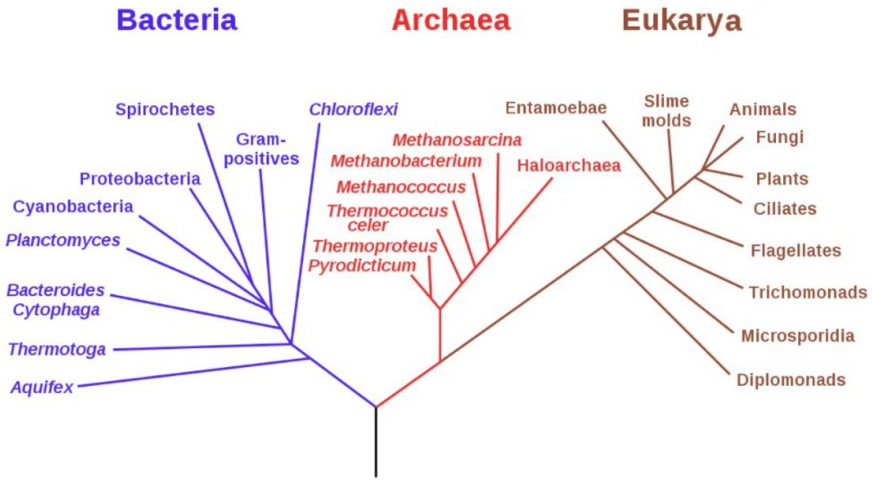

Figure 1. The universal phylogenetic tree in rooted form, showing the three domains of the Tree of Life. Adapted from [5].

Archaea and Bacteria constitute the so-called "prokaryotes", i.e., single-celled organisms that do not have a nucleus separating their genetic material from the rest of the cell. Almost all prokaryotes have a cell wall, i.e., a protective structure that allows them to survive in extreme conditions, which is located outside of their plasma membrane. However, there are differences between Bacteria and Archaea. Although both Bacteria and Archaea have cell membranes containing a hydrophobic portion, in the case of Bacteria, the cell membrane is composed of peptidoglycan, a complex of protein and sugars, whereas in the case of Archaea, it is composed of polysaccharides. In contrast, Eukarya includes both unicellular and multicellular organisms that possess nuclei to enclose their DNA apart from the rest of the cell [9].

In connection with the subject matter of the present review, it is useful to premise some aspects of Fe-S clusters in biology. For example, Figure 2 schematically illustrates the structures of the most common biological iron-sulfur (Fe-S) clusters.

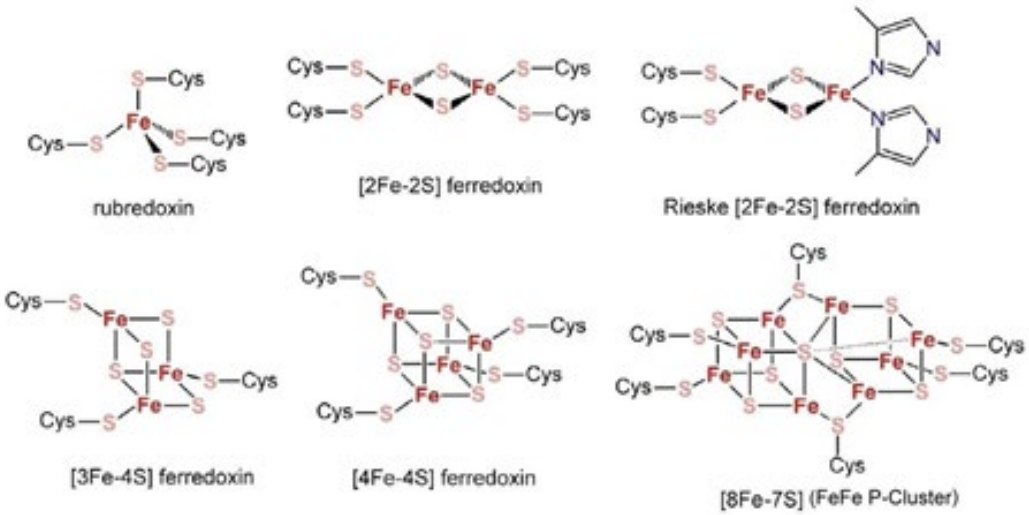

Figure 2. The canonical forms of biological Fe-S clusters. Reprinted from [10].

In general, Fe-S clusters act as redox-active cofactors of specific enzymatic reactions carried out by many proteins [11–21]. In this picture, after having reviewed the structure and electrochemistry of Fe-S clusters of different nuclearity [10,22–31], we now devote our attention to the fundamental role of [2Fe-2S] centers in activating a wide spectrum of enzymatic reactions. In addition we have reported about the role of prebiotic iron–sulfur peptide catalysts in triggering pH gradients exploited by all known living organisms [32].

As in our previous papers, this discussion was exclusively limited to those proteins whose molecular structure has been ascertained by X-ray crystallography, NMR spectroscopy, or cryo-electron microscopy. (Unless otherwise specified, all images pertinent to the molecular architecture of the different species have been obtained by the NGL Viewer.)

Since we have already dealt with structure and electrochemistry of metalloproteins hosting "classical" ($[Fe_2S_2](S^{\gamma}_{Cys})_4$) and Rieske-type $[Fe_2S_2](Cys)_2(His)_2$ ferredoxins [23] as well as "non-classical" $[Fe_2S_2](Cys)_3(X)$ (X = Asp, Arg, His) [24] ferredoxins, we did not consider them herein.

2. Archaeal Enzymatic Reactions

2.1. Archaeoglobus fulgidus

Archaeoglobus fulgidus is a member of the sulphate reducers Archaeoglobales that grow organoheterotrophically between 60 °C and 95 °C, with optimum growth at 83 °C using a variety of carbon and energy sources as well as lithoautotrophically on hydrogen, thiosulphate, and carbon dioxide [33,34]. It is involved in the two [2Fe-2S]-containing biological functions "Copper chaperone CopZ" and "Cysteine desulfurase".

2.1.1. Copper Chaperone CopZ

Copper is an absolutely required metal by living systems, but it is potentially toxic to cells; therefore, the intracellular movement of this metal inside copper-dependent proteins is fundamental to normal cellular metabolism. As a matter of fact, copper ions act as cofactors in many enzymes (namely: Cu, Zn superoxide dismutase, cytochrome c oxidase, amino oxidase, galactose oxidase, dopamine β-hydroxylase, peptidylglycine α-hydroxylating monooxygenase, tyrosinase, lysyl oxidase, galactose oxidase, methane monooxygenase, catechol oxidase, ceruloplasmin and laccase) [35].

In this picture, copper chaperones are deputed to avoid the presence of free Cu^+ levels in cells by performing the dual functions of trafficking (i.e., binding and delivering copper ions to intracellular compartments and inserting them into the active sites of specific copper dependent enzymes) and preventing the toxic effects of over-exposure to copper ions in transit. In fact, the Cu(II)/Cu(I) redox cycling is a fundamental requirement for single electron transfer reactions in copper-containing enzymes and proteins, but such a redox cycle contributes to the formation of hydroxyl radicals and subsequent oxidative damage to cellular components (DNA, proteins, lipids, and so on) in that copper ions can initiate hydroxyl radical formation in solution when exposed to superoxide anion and hydrogen peroxide in a Fenton-like reaction (the "Fenton" reaction deals with the biological damage caused by hydrogen peroxide and iron ions [36,37]) [38–41].

It is noted that the copper toxicity is also bound to its capacity to damage proteins containing Fe-S clusters by displacing the pertinent iron atoms followed by its coordination to the decomplexed sulfur ligands [42].

P-type ATPases are ion pumps that carry out many fundamental processes in biology and medicine, particularly the removal of toxic ions from cells, making use of the energy stored in ATP to transport specific ions across the cell membrane against a concentration gradient. Taking into account that P-ATPases are divided into five main classes, P1, P2, P3, P4, and P5, which, in turn, are subdivided in subfamilies (P1A, P1B, and so on [43–45]), in Cu^+-ATPases, metal binding to transmembrane metal-binding sites (TM-MBS) is required for enzyme phosphorylation and subsequent transport provided that Cu^+ is bound to a chaperone protein [46]. In fact, Cu^+ chaperones transfer Cu^+ ions to regulatory cytoplasmic metal-binding domains (MBDs) present in Cu^+-ATPases.

A relatively high number of copper chaperones exist, but the simplest example of chaperoned copper delivery is represented by the copper efflux chaperone CopZ and the copper-transporting ATPase CopA [47,48].

Archaeoglobus fulgidus encodes a putative CopZ copper chaperone that contains an unusual cysteine-rich N-terminal domain of 130 amino acids in addition to a C-terminal copper-binding domain with a conserved CXXC motif. The N-terminal domain (CopZ-NT) crystallizes as a monomer that contains a classical ferredoxin-like [2Fe-2S] cluster (Figure 3) [49].

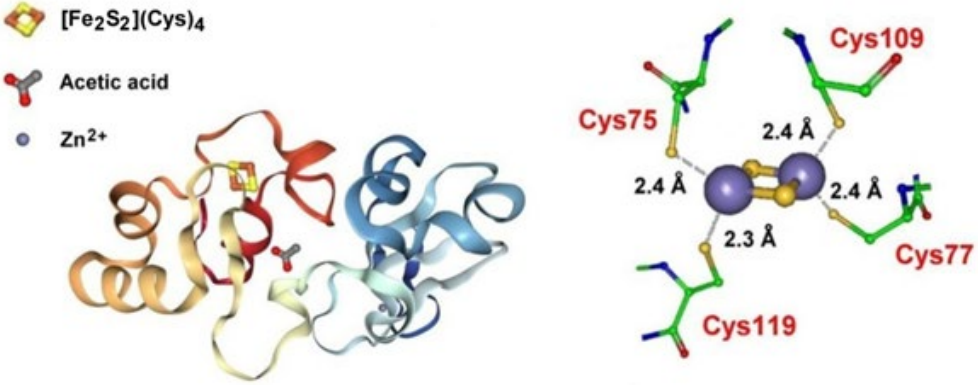

Figure 3. The molecular structure of *Archaeoglobus fulgidus* CopZ-NT, together with the composition of its [2Fe-2S] cluster. Adapted from [49]; [PDB 2HU9].

Attempts to explain the complex mechanism of the delivery of Cu^+ by the Cu^+ chaperone CopZ to the corresponding Cu^+-ATPase CopA (which is a member of the P1B subgroup of P-type ATPases) have been carried out [36,48,49]. In short, it has been proposed that reduced CopZ-N can reduce, eventually exploiting the redox activity of the vicinal [2Fe-2S] cluster, Cu(II) to Cu(I), which is then transferred to the CopZ C-terminal domain (CopZ-C) and then delivered to CopA that effluxes it from the cell.

At the moment, no redox data are available for the $[2Fe\text{-}2S]^{2+/+}$ transition, but aiming to support such a mechanism, the fact that the $[2Fe\text{-}2S]^{2+}$ is reduced by dithionite [50] seems to suggest a potential value lower (i.e., less negative) than −0.5 V (vs. NHE)) for such an electron transfer (in fact, taking into account that the reduction potential of dithionite is conditioned either by pH and dithionite itself, a value less negative than −0.5 V vs. NHE is commonly estimated in the pH range from 7 to 9 [51]); thus, given such a physiological value, it sounds plausible that Cu(II) might be reduced to Cu(I) through the $[2Fe\text{-}2S]^{+/2+}$ oxidation.

2.1.2. Cysteine Desulfurase

It is known that Fe-S clusters are ubiquitous cofactors crucial for the existence of life on Earth. Their synthesis in vitro looks like to be a relatively simple task by using free iron ions, sulfides, and suitable ligands under proper conditions and then transferring them to a proper protein without enzymatic assistance [52], but their in vivo biogenesis appears rather intricate. Plausible hypotheses about how such cofactors could be transferred within the cellular environment began to take hold in the 1990s (a few recent citations include [53–71]). It is, however, difficult to give a mechanism for Fe-S biosynthesis valid for the three domains, i.e., Archaea, Bacteria, and Eukarya. In Bacteria, three distinct distinct machineries catalyze the biosynthesis of [Fe-S] clusters and their transfer to target proteins: (i) the NIF (Nitrogen Fixation) system; (ii) the ISC (Iron Sulfur Cluster) system; and (iii) the sulfur mobilization SUF system [72,73]. In general, the biosynthetic pathway is constituted by two basic processes: "*assembly*" and "*transfer*". In the "assembly" stage, a scaffold protein (SufB) receives sulfur and iron from unknown donors and builds Fe-S clusters; in the "transfer" stage, an ATPase (SufC) facilitates the release of Fe-S clusters from the scaffold SufB, and then the Fe-S clusters are transported to target apoproteins *via* different carrier proteins [70]. This means that the biosynthetic pathways in Bacteria and Eukarya are quite proven (see, for instance, [63,69,70,74–76]). In contrast, the Fe-S biogenesis in Archaea is not yet accurately known [76–78], even if a few SUF systems are there distributed [79–81]. Premised that L-Cysteine desulfurase IscS and scaffold IscU proteins are universally involved in Fe/S cluster synthesis, in Archaea, the cysteine desulfurase provides one ligand for the binding of an Fe-S cluster. One of the central components in the case of the ISC system is IscS, a pyridoxal-5′-phosphate (PLP)-dependent desulfurase that uses L-cysteine as a substrate to generate a persulfide on its active site cysteine. The activated sulfane sulfur is subsequently reductively delivered to the second central component of ISC, the scaffold protein IscU, where [Fe-S] clusters are assembled [72]. In particular, the *Archaeoglobus fulgidus* genome encodes proteins having a high degree of primary structure similarity to IscS and IscU from other organisms. However, its IscS is unusual because it lacks the active site lysine residue that normally forms an internal Schiff base with pyridoxal-phosphate (PLP) and serves as a base during catalysis [73]. It must be also taken into account that in Archaea, cysteine is not the sulfur source for iron-sulfur clusters; in fact, the sulfur does not originate from cysteine, but it is derived from sulfide, which is abundant in the anaerobic environment where the organism was isolated [80].

In this context, Figure 4 shows the different components still lacking for a sufficiently complete description of the Archaeal biosynthetic pathway [81].

For example, in Bacteria and Eukarya, the alternative ApbC (pyrimidine biosynthetic protein C) binds and rapidly transfers [Fe-S] clusters to an apoprotein [81–83].

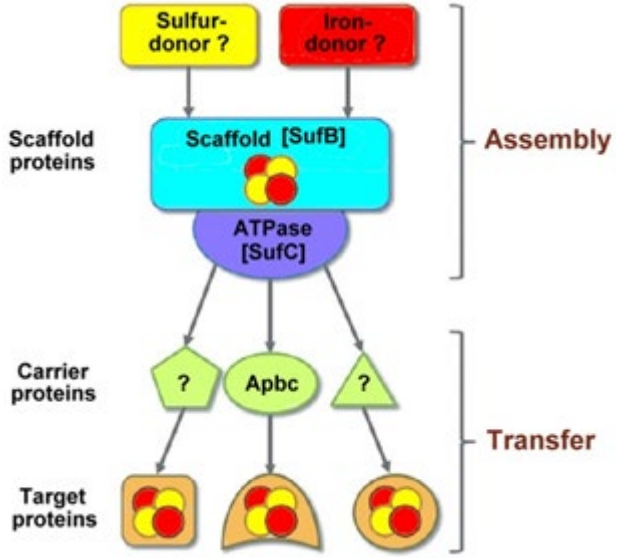

Figure 4. A model of Fe-S cluster biogenesis in Archaea. Adapted from [81].

In this picture, *Archaeoglobus fulgidus* is able to express two different complexes that should be potentially expected to exhibit *desulfurase* activity. The first complex is constituted by the anaerobically purified dithiothreitol (DTT)-treated αβ heterodimer $(IscU\text{-}IscS)_2$, which hosts a classical $[Fe_2S_2(Cys)_4]$ active site, in which Cys33, Cys58, and Cys102 belong to the IscU system, whereas Cys321 comes from the IscS system (Figure 5) [84].

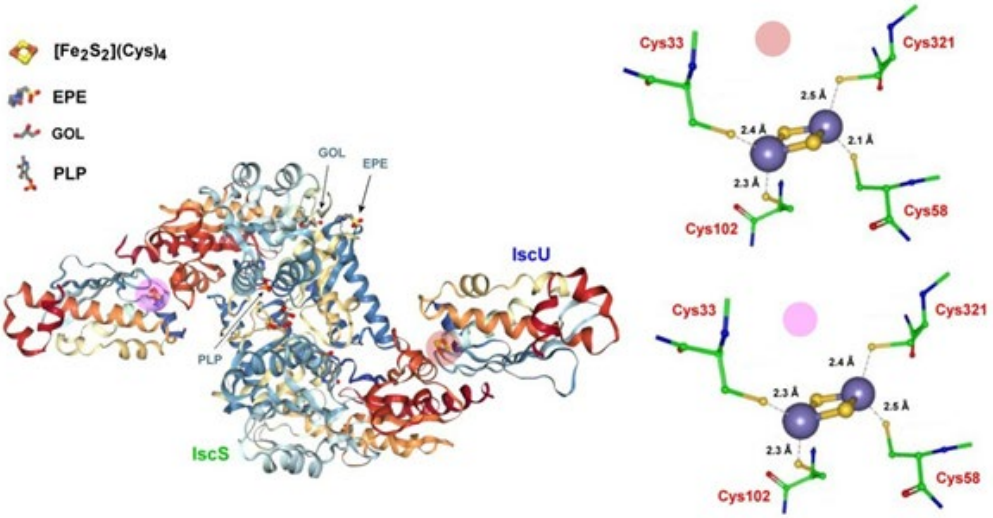

Figure 5. Crystal structure of the active site of the heterotetrameric holo complex $(IscS\text{-}IscU)_2$ protein of *Archaeoglobus fulgidus* and the pertinent Fe-S cluster (there are two slightly different isoforms of the [2Fe-2S] clusters). EPE = 4-(2-hydroxyethyl)-1- piperazine ethanesulfonic acid; GOL = glycerol; PLP = pyridoxal-5′-phosphate. The location of the Fe-S clusters location is evidenced by colored disks. Adapted from [84]; [PDB 4EB5].

The redox potential of the $[2Fe\text{-}2S]^{2+/+}$ transition of the two clusters is not available.

Since it is known that the replacement of Asp for Ala in IscU systems stabilizes the $[Fe_2S_2]$ rhomb [85], the Asp35 residue has been replaced by Ala affording the $(IscS\text{-}IscU^{D35A})_2$ complex [84]. Such a mutation, however, causes the loss of its cysteine desulfurase activity. In fact, while in $(IscS\text{-}IscU)_2$, the Schiff base-forming Lys residue is associated with the pyridoxal-5′-phosphate (PLP) enzyme, and in the new complex the Asp35Ala mutation makes the Schiff base-forming Ala residue associate with pyridoxamine-5′-phosphate (PMP), which is not catalytically active in cysteine desulfurase [86,87]. Such a second

complex is constituted by the air-exposed $\alpha_2\beta$ heterotrimer ($[Fe_2S_2]$-IscS-$IscU^{D35A}$)$_2$ shown in Figure 6 [84].

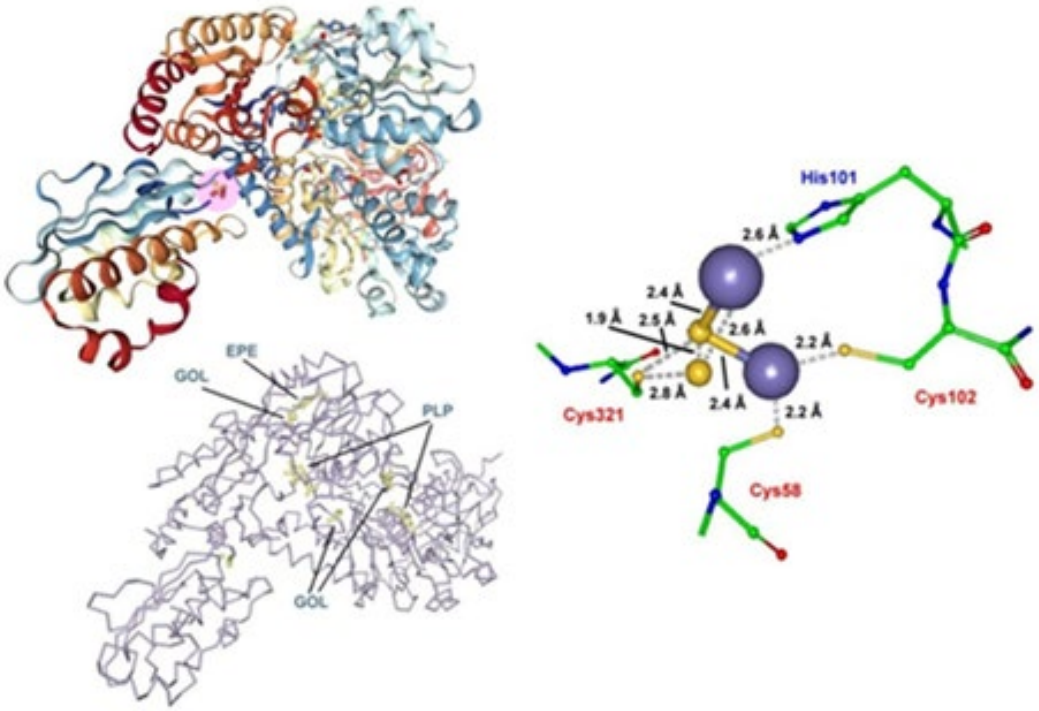

Figure 6. The molecular geometry of the air-exposed heterotrimeric form of *Archaeoglobus fulgidus* ($[Fe_2S_2]$-IscS-$IscU^{D35A}$)$_2$ complex. The iron sulfur cluster hosts an unusual active site in which the release of a sulfide atom from the [2Fe-2S] rhomb occurs. About the terms PLP, EPE, and GOL, see Figure 5. Adapted from [84]; [PDB 4EB7].

As seen, the [2Fe-2S] cluster has a markedly unusual geometry.

Additionally, in this case, no redox data are available for such a Fe-S center.

In confirmation of the stabilization of the $[Fe_2S_2]$ cluster played by the Asp35Ala mutation, the mutation Asp199Lys in *Archaeoglobus fulgidus*, lacking the presence of Ala, does not allow such a mutation to contain any $[Fe_2S_2]$ cluster [86,87].

As above mentioned, the NIF (Nitrogen Fixation), ISC (Iron Sulfur Cluster), and SUF (Sulfur Formation) systems catalyze the biosynthesis of [Fe-S] clusters and their transfer to target proteins [69]. In particular, the ISC machinery is the only essential function of mitochondria actually identified and is required not only for the maturation of mitochondrial Fe-S proteins but also for the formation of Fe-S clusters in other cell compartments [88]. Archaea must have a mechanism to assemble Fe-S clusters, but many members lack homologs of the known bacterial and eukaryotic Nif or Isc systems, suggesting that an alternative system is present (e.g., "the evolution of SUF operons in Archaea and Bacteria" in [70]; "the taxonomic distribution of the ABC ATPase of SufB and SufD in Archaea and Bacteria" in [80]; "the archaeal basal machinery of transcriptional repression" in [89]; "the archaeal phylogeny" in [90]; "the archaeal DNA replication machinery" in [91,92]; "the unique archaeal cell division machinery" in [93]; "the SUF machinery is the only Fe-S cluster biosynthesis system conserved in some aerobic and hyperthermoacidophilic Archaea" in [94]; "the core machineries that copy DNA are conserved in all three domains of life" in [95]; "nanobiomotors of archaeal DNA repair machineries" in [96]; "RNA processing machineries in Archaea" in [97]).

It is therefore useful to look at the ISC machineries of Bacteria, Eukarya, and in part of Archaea.

Figure 7 illustrates the pathway of the eukaryotic ISC machinery [98].

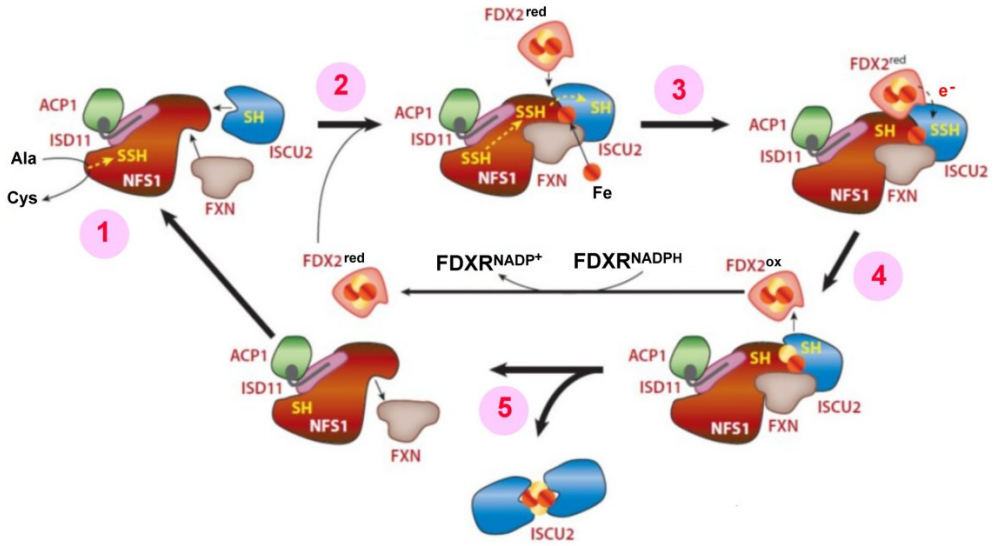

Figure 7. Hypothetical mechanism of [2Fe-2S] cluster synthesis by and structure of the eukaryotic core ISC complex. Adapted from [98].

De novo [2Fe-2S] cluster synthesis on the mitochondrial scaffold protein ISCU2 depends on six additional ISC proteins: the desulfurase complex NFS1 (a protein that catalyzes the removal of elemental sulfur from cysteine to produce alanine, thus supplying the inorganic sulfur for iron-sulfur Fe-S clusters), ISD11 (the cysteine desulfurase activator (YER048W-A)) with dynamically associating ACP1 (the enzyme acid phosphatase 1 removes phosphate from other molecules during digestion and catalyzes the conversion of orthophosphoric monoester and H_2O to alcohol and phosphoric acid), frataxin (FXN), ferredoxin (FDX2), and its reductase (FDXR). The synthesis pathway can be divided into five subreactions. (**1**) The NFS1 generates a persulfide (−SSH) on its conserved active-site cysteine residue by converting free cysteine to alanine, a reaction assisted by FXN. (**2**) The persulfide is then transferred on the flexible Cys loop from the catalytic site of NFS1 close to PLP to the surface of NFS1, a reaction assisted by FXN. (**3**) After iron binding to ISCU2, the NFS1-linked persulfide sulfur is transferred to one of the conserved Cys residues of the scaffold. (**4**) The transient binding of reduced FDX2 (FDX2red) to NFS1–ISCU2 promotes reduction (e^-) of the persulfide sulfur on ISCU2 and generates sulfide (S^{2-}) present in Fe-S clusters (**5**). How a potential Fe-S intermediate protein is formed and further converted to a [2Fe-2S] cluster is unknown. At any rate, the oxidized FDX2 (FDX2ox) leaves the complex and is reduced by its reductase FDXR and NADPH to FDX2red. The final product of the reaction cycle may be a dimer of ISCU2 with a bridging [2Fe-2S] cluster, as revealed by biochemical reconstitution [93].

Figure 8 depicts the pathway of the bacterial ISC machinery [74].

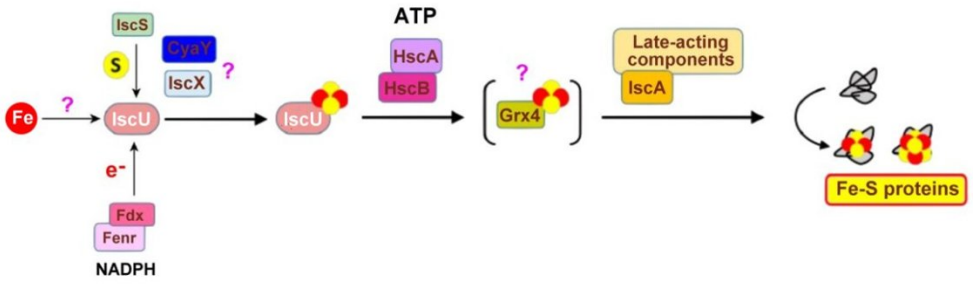

Figure 8. Main components of the bacterial ISC machinery. Adapted from [74].

As illustrated, the bacterial ISC machinery encompasses proteins encoded by the ISC operon: IscU (the scaffold protein), IscS (the L-cysteine desulfurase), IscX (a puta-

tive regulator of the activity of IscS and IscR (a transcriptional regulator of the whole operon), Fdx (ferredoxin), and HscA (a specialized Hsp70 chaperone. HscA, as other Hsp70 (70-kilodalton shock proteins), has general chaperone-like activities (prevention of aggregation and protein folding assistance). HscB stimulates the ATPase activity. IscA has also been proposed as a scaffold for the iron-sulfur cluster assembly, CyaY (frataxin) and Fenr (ferredoxin reductase). Grx4 may function as a relay to late-acting components, among which are the IscA proteins that have specialized functions in the assembly of [4Fe4S] clusters and/or insertion of [2Fe-2S] and [4Fe-4S] clusters into recipients' enzymes. Recently, it has been demonstrated that the mitochondrial [4Fe-4S] protein assembly involves reductive [2Fe-2S] cluster fusion on the A-type (ISCA1-ISCA2) by electron flow from ferredoxin FDX2 [99].

In addition, in order to account for the maturation of housekeeping Fe-S proteins (to become the holo form), Bacteria use one or both the ISC and SUF machineries in parallel (Figure 9) [100].

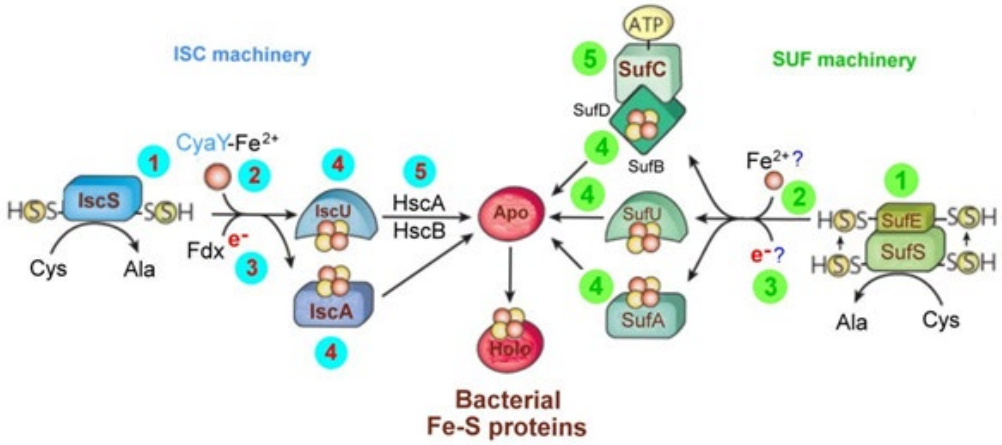

Figure 9. Bacteria in the Fe-S protein biogenesis can exploit the ISC and SUF machineries. Adapted from [100].

The ISC machinery (left part, light blue in color) consists of the cysteine desulfurase IscS (**1**) which liberates the yellow circled sulfur from cysteine, generating an IscS-bound persulphide (−SSH) on a conserved cysteine residue. A transient Fe-S cluster is formed on the scaffold proteins IscU and/or IscA. The synthesis of *de novo* Fe-S cluster **(2)** involves the transfer of iron (red circle) from the iron-binding protein CyaY (frataxin) and other yet-unknown factors. The ferredoxin (Fdx) plausibly serves to reduce the sulfur in cysteine to sulfide (**3**). The transiently bound Fe-S cluster is then transferred from the IscU/IscA scaffolds (**4**) to apoproteins (Apo) for coordination with specific residues (usually cysteine or histidine). Transfer from IscU is provided by the dedicated chaperone systems HscA and HscB (**5**).

The ISC machinery is operative under normal conditions, whereas the SUF machinery (green colored, right part) is active under oxidative-stress and iron-limiting conditions. In this case, biogenesis is initiated by the cysteine desulfurase SufS (**1**), which functions comparably to IscS except that the sulfur is first transferred to a conserved cysteine residue of SufE (**1**) and bound as a persulfide. Putative iron and electron donors in this system are still unknown (**2, 3**). Three components might be scaffolds for de novo Fe-S cluster assembly: SufU and SufA (**4**), which show similarities to IscU and IscA, respectively, and SufB (**4**), which forms a stable complex with SufB-SufC (**5**). SufrC is an ATPase and may facilitate Fe-S cluster dissociation from SufB and subsequent transfer to apoproteins.

Among the above-cited archaeal machineries, Figure 10 illustrates the role played by the SufBC2D complex in the archaeal Fe-S biosynthesis [16,80].

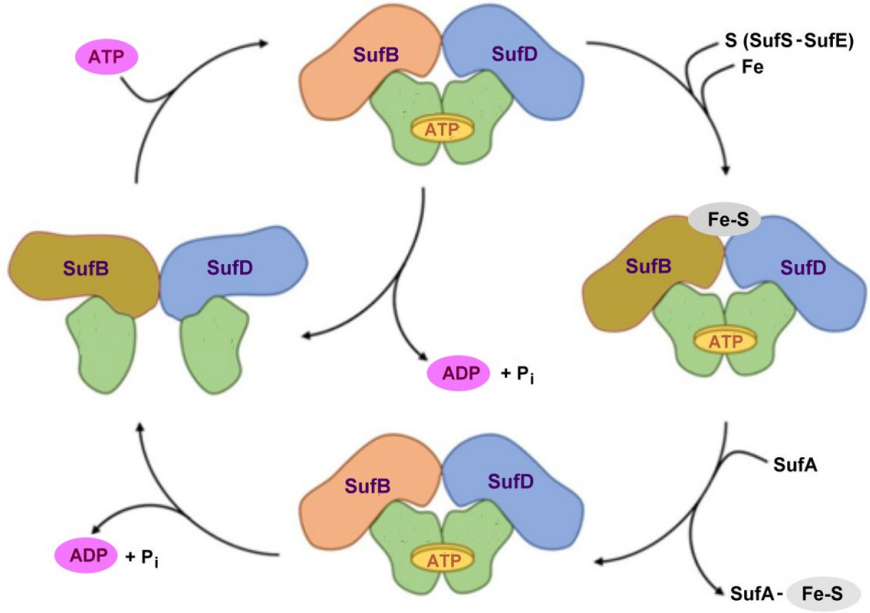

Figure 10. The proposed mechanism played by the SufBC2D complex in archaeal Fe-S biogenesis. Adapted from [80].

2.2. Methanothrix thermoacetophila

The Z-517 strain of *Methanothrix thermoacetophila* is an anaerobic, thermophilic archaeon originally isolated from mud of thermal Khlorid Lake in Kamchatka [101]. In reality, such an archeon as isolated from anaerobic digester sludge is also known as *Methanosaeta thermophila* with references to strains DSM 6194/JCM 14653/NBRC 101360/PT [102–104].

The IscU System

In Section 2.1.2, speaking about cysteine desulfurase, we already discussed the IscU system in Fe-S biogenesis.

The IscU wild type from *Methanothrix thermoacetophila* (*Mt* IscU WT) crystallizes as a homodimer (Figure 11) [105].

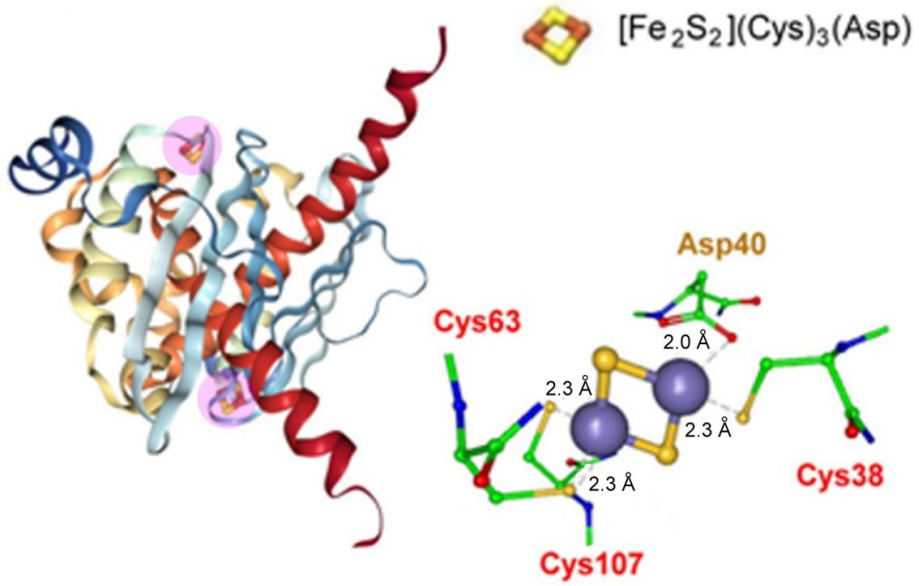

Figure 11. Overall structure of the dimeric *Mt* IscU WT, together with a few structural details of the pertinent [2Fe-2S] cluster. Adapted from [105]; [PDB 7C8M].

EPR spectroscopic analysis proves that in solution two adjacent [2Fe-2S] clusters in the wild-type dimer are converted to a [4Fe-4S] cluster via reductive coupling [105].

Additionally available are the crystal structures of the variants *Mt* IscU H106A [105; PDB 7C8N] and *Mt* IscU H106C [106; PDB 7CNV], as well as that of the double-variant *Mt* IscU D40A/H106A [105; PDB 7C8O].

In contrast with *Mt* IscU WT, the *Mt* IscU H106A variant prevents the 2[2Fe-2S]/[4Fe-4S] conversion, suggesting that the H106 fragment provides a key feature of such a conversion [105].

However, the molecular structure of the variant *Mt* IscU H106C, illustrated in Figure 12, deserves some attention [106].

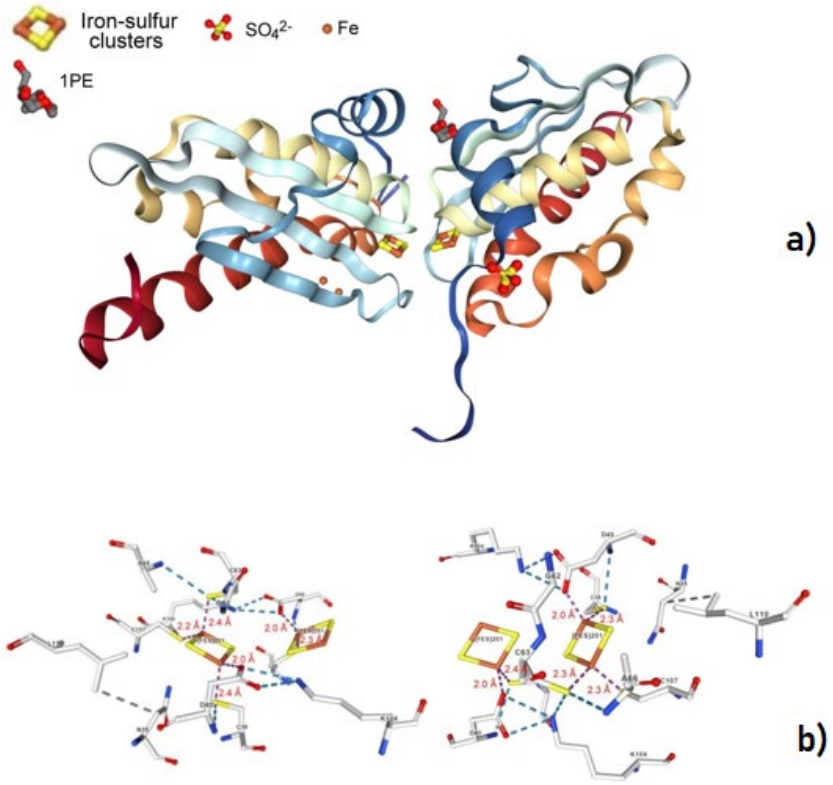

Figure 12. Overall structure of the dimeric *Mt* IscU H106C (**a**), and a cartoon representation of the pertinent iron-sulfur clusters (**b**). Adapted from [106]; [PDB 7CNV, to be published].

We naively think that, while in the case of H106A, the replacement of the positively charged and polar hydrophilic His106 for the non-polar hydrophobic Ala, compensating each other, leaves the surficial water affinity unchanged, in the case of H106C, the replacement of the positively charged and polar hydrophilic His106 for the uncharged and non-polar hydrophilic Cys mutates the surficial water affinity insertion, causing, at least in part, the unusual structural complexity of the outlined Fe-S clusters.

2.3. Pyrobaculum calidifontis

Pyrobaculum calidifontis is a facultatively aerobic, heterotrophic, hyperthermophilic archaeon isolated from a terrestrial hot spring in the Philippines that grows optimally from 90 °C to 95 °C and pH 7.0 in atmospheric air [107]. It is involved in two [2Fe-2S]-containing biological functions: "CRISPR-associated exonuclease Cas4" and "Zinc finger, CDGSH-type domain proteins", respectively.

2.3.1. CRISPR-Associated Exonuclease Cas4

The Clustered Regularly Interspaced Short Palindromic Repeats-Cas (i.e., CRISPR-associated) system is an adaptive-immunity prokaryotic defense apparatus with a mul-

titude of unknown genes comprising up to 45 novel protein families. This immunity system is based on the incorporation of short DNA sequences (30–50 nucleotides) from viral genomes or plasmids into the host chromosome, which are then transcribed into guide RNAs (CRISPR RNAs or crRNAs) and direct Cas proteins to specifically degrade DNAs or RNAs containing the complementary sequences. CRISPR immunity has been categorized into three stages: "adaptation", "expression", and "interference". During the adaptation stage, new spacer sequences are incorporated into the CRISPR locus. During the expression stage, the CRISPR locus is transcribed to generate, or mature, the CRISPR RNA (crR-NA). Finally, in the interference stage, the crRNA bound to Cas proteins is employed as the guide to recognize the protospacer or a closely similar sequence in an invading ge-nome of a virus or plasmid that is then cleaved and inactivated by Cas nuclease(s). All CRISPR-Cas systems are divided into two distinct classes on the basis of the design principles of the effector modules: Class 1 systems have multi-subunit effector complexes com-prising several Cas proteins; Class 2 systems have the effector as a single, large, mul-tidomain protein. In turn, Class 1 is divided into types I, III, and IV, whereas class 2 is divided into types II, V, and VI. Each type is further classified into multiple subtypes that are distinguished by subtle differences in locus organization, leading to 13 families of core Cas proteins: Cas1 and Cas2, which form the adaptation complex that is universal to all autonomous CRISPR-Cas systems; Cas3, which is a helicase that typically contains a nuclease domain and is involved in target cleavage in type I systems; Cas4, which is an endonuclease required for adaptation in many CRISPR-Cas variants; Cas5, Cas6, and Cas7, which are distantly related members of the so-called RAMP domain superfamily; Cas8, which is an enzymatically inactive large subunit of type I effector complexes; Cas9, which is a type II effector nuclease and contributes to spacer acquisition; Cas10, which is a large subunit of type III effector complexes and contains a Palm domain homologous to those of DNA polymerases and nucleotide cyclases; Cas11, which is a small subunit of the type I and type III effector complexes; Cas12, which is an effector endonuclease of type V; and Cas13, which is an effector RNase of type VI [108–112]. CRISPR-Cas systems provide microorganisms with adaptive immunity by employing short sequences, termed spacers, that guide Cas proteins to cleave foreign DNA [113,114].

As shown in Figure 13, *Pyrobaculum calidifontis* Cas4 hosts a classical $[Fe_2S_2(Cys)_4]$ cluster [115].

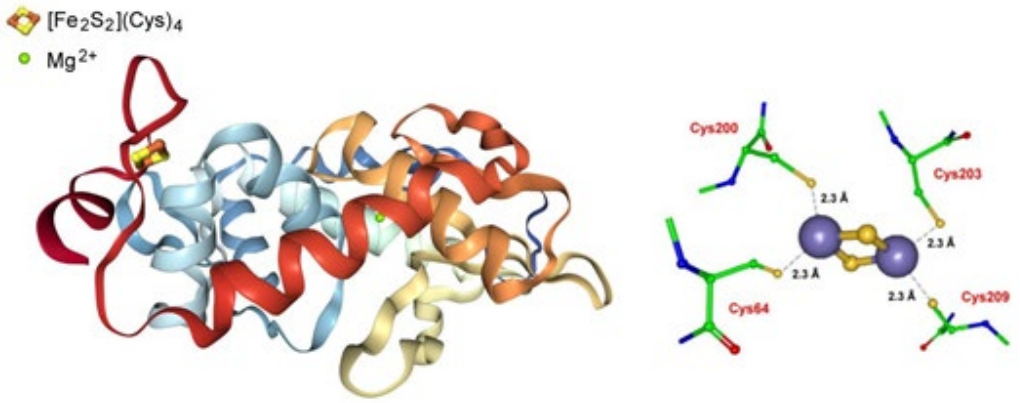

Figure 13. Crystal structure of the monomeric CRISPR-associated Cas4 protein Pcal_0546 from *Pyrobaculum calidifontis*. Adapted from [115]; [PDB 4R5Q].

To our knowledge, no redox data are available about the redox properties of the [2Fe-2S] center. Nevertheless, the role of such cluster in the kinetics of CRISPR-associated Cas4 protein is not yet understood. What is known is that, as far as the nuclease activity of the protein is concerned (i.e., catalysis of the hydrolysis of ester linkages within nucleic acids), the [2Fe-2S] center does not seem to be determinant given that its disruption (by alanine replacement of the coordinating Cys residues) has no negative effect [115].

2.3.2. Zinc Finger, CDGSH-Type Domain Proteins

The CDGSH (C-D-G-(S/A/T)-H) domains (CISDs) are classified into seven major types [116,117]. Such domains are found in proteins from a wide range of organisms (with the exception of fungi) and its peculiar feature is the conserved aminoacid sequence [C-X-C-X2-(S/T)-X3-P-X-C-D-G-(S/A/T)-H] (the Ser residue can be replaced by Ala or Thr). Such a typical domain binds a redox-active pH-labile [2Fe-2S] cluster.

Pyrobaculum calidifontis contains a type 3 CISD that crystallizes in a homodimeric form hosting a non-classical $[Fe_2S_2](Cys)_3(His)$ ferredoxin (Figure 14).

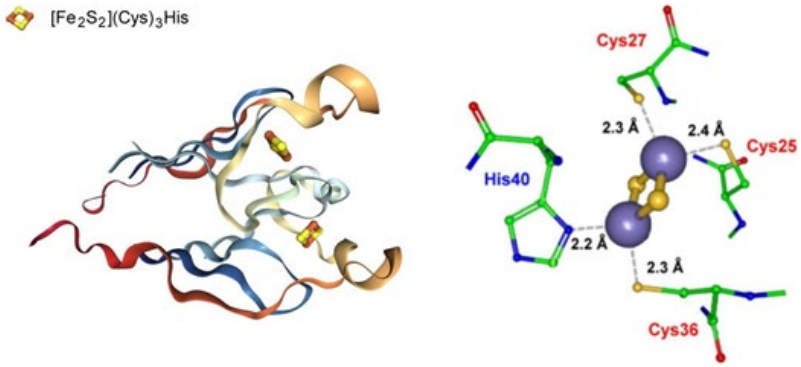

Figure 14. The molecular structure of *Pyrobaculum calidifontis* type 3 CISD together with that of the hosted [2Fe-2S] clusters. Adapted from [116]; [PDB 3TBO].

No redox data are available for such a Fe-S cluster.

2.4. Pyrococcus horikoshii

Pyrococcus horikoshii is an anaerobic archaebacterium isolated in 1992 from a hydrothermal vent at a depth of 1395 m in the Okinawa Trough in the Pacific Ocean that grows at temperatures ranging from 85 °C to 105 °C and optimally at 98 °C [118,119]. It is able to express a [2Fe-2S] center that plausibly arises from degradation of the [4Fe-4S] cluster catalytically active in "tRNA-5-methyluridine(54) 2-sulfurtransferase".

tRNA-5-methyluridine(54) 2-sulfurtransferase

The biosynthesis of transfer RNA (tRNA) sulfur modifications involves unique sulfur trafficking systems that are closely related to cellular sulfur metabolism and "modification enzymes" that incorporate sulfur atoms into tRNA. tRNA is an essential adaptor molecule that bridges genomic information from mRNAs to amino acid sequences in proteins [120].

The enzyme tRNA-5-methyluridine(54) 2-sulfurtransferase catalyzes the ATP-dependent 2-thiolation of 5-methyluridine residue at position 54 in the T loop of tRNAs, leading to 5-methyl-2-thiouridine (m5s2U or s2T) (Figure 15) [121].

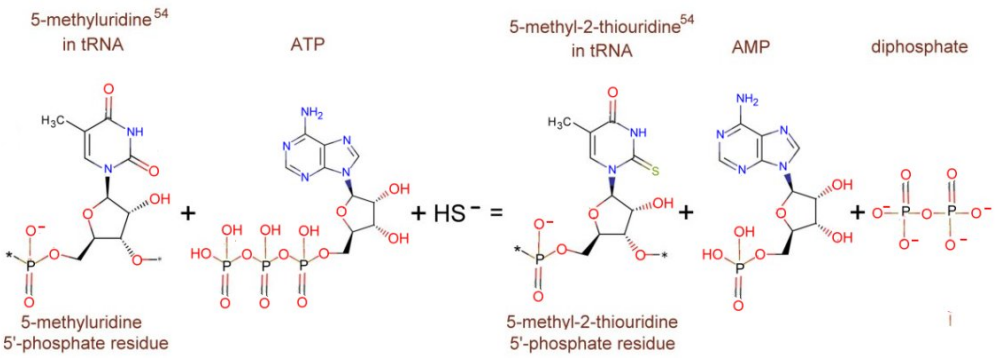

Figure 15. The reaction catalyzed by tRNA-5-methyluridine(54) 2-sulfurtransferase. Adapted from [121,122].

The simple nonredox substitution of the C2-uridine carbonyl oxygen by sulfur is catalyzed by tRNA thiouridine synthetases, called TtuA. Spectroscopic, enzymatic, and structural studies indicate that TtuA, a representative member of a tRNA modification enzyme superfamily, carries a catalytically essential [4Fe-4S] cluster and requires ATP for activity.

Figure 16 illustrates the crystal structures of the [4Fe-4S] cluster (a) as well as that of the degraded [2Fe-2S] cluster (b) [122].

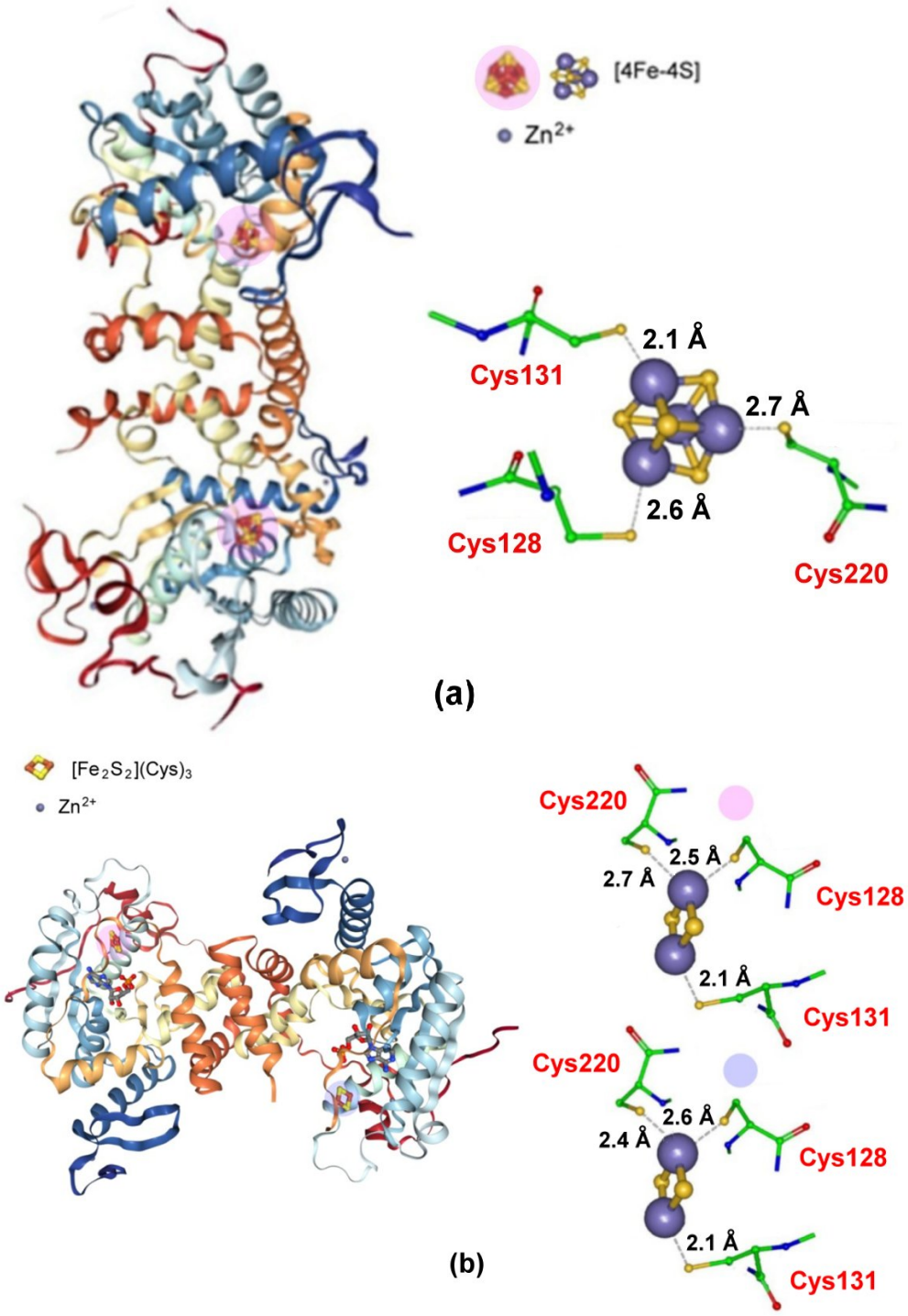

Figure 16. Molecular architectures of the homodimers of *Pyrococcus horikoshii* TtuA together with the geometries of the Fe-S clusters expressed by: (**a**) the catalytically active species (adapted from [124; PDB 5MKQ]); (**b**) its degraded form (adapted from [122]; [PDB 5MKO]).

As shown, the [2Fe-2S] cluster of the degraded form crystallizes in two slightly different isoforms, neither of which have been electrochemically investigated. It is noted that the three cysteine ligands present in the active [4Fe-4S] cluster reorganize maintaining the same coordination in the degraded [2Fe-2S] cluster. It has also been found that the fourth uncoordinated Fe of the [4Fe-4S] site may bind a small ligand, such as exogenous sulfide, thus acting eventually as a sulfur carrier [122]; [PDB 5MKP].

No redox potential values are available for both the Fe-S clusters.

2.5. Sulfolobus acidocaldarius

The bacterium *Sulfolobus acidocaldarius* was first isolated from a variety of thermal acid environments by enrichment at elevated temperatures (from 45 °C to 70 °C) and low pH (from 2.0 to 6.0) [123,124]. In contrast, at ambient conditions, it maintains an intracellular pH of about 5.8–6.5; thus, thanks to a respiration-driven proton extrusion process [125], a dramatic pH gradient occurs [126].

The Respiratory System

Since 1985, the respiratory properties of *Sulfolobus acidocaldarius* seemed to depend energetically on respiration-coupled phosphorylation in that its ATP content strictly depended on respiratory activity. Its membrane is capable of proton pumping and presumably contains a branched electron transport system based on different cytochromes and the presence of a terminal oxidases directly related to the redox aptitude of *Caldariella* quinone [127]. Hereafter, as below-discussed, the crucial respiration features were better and better defined.

Sulfolobus acidocaldarius is able to express two alternative cytochrome oxidase complexes:

1. The SoxABCD complex (that acts as a proton pump in reconstituted in vitro system [128] as well as in vivo [129]) with its subunits SoxA (no prostethic group), SoxB, and SoxC (both having the prostethic group cytochrome A_s (the pedice S means *Sulfolobus*) [130,131]), and SoxD (we do not deal with SoxABCD as it does not contain any Fe-S cluster; for more details about such a cytochrome oxygenase, see reference [131]).
2. The SoxM complex constitutes a unique respiratory supercomplex combining features of a cytochrome bc_1 complex (subunits SoxF, SoxG, and SoxE) and cytochrome *c* oxidase (subunits SoxM, SoxH, and SoxL). In fact, SoxM hosts two cytochrome-*b* types, namely *b* and b_3, that constitute a quinol bb_3 oxidase [132]), where cytochrome *b* encodes a Cu_A site located in the subunit II (SoxH) typical of cytochrome *c* oxidase that constitutes the primary electron acceptor (it is probably linked to two histidines, a cysteine and a methionine of cupredoxin [133]) and the cytochrome b_3 that is coupled to a Cu_B center that catalyzes the dioxygen reduction to two water molecules, thus completing the cellular respiration process [134]; in fact, SoxH bears a prostethic group Cu_A that resides in subunit II of cytochrome *c* oxidase and hosts two heme As. SoxF hosts a iron-sulfur protein II. SoxE bears the blue copper centre sulfocyanin, and finally SoxI hosts an iron-sulfur protein I.

There are few examples that illustrate the components and their main electron-transport functions of the SoxM oxidase [134–137] (Figure 17).

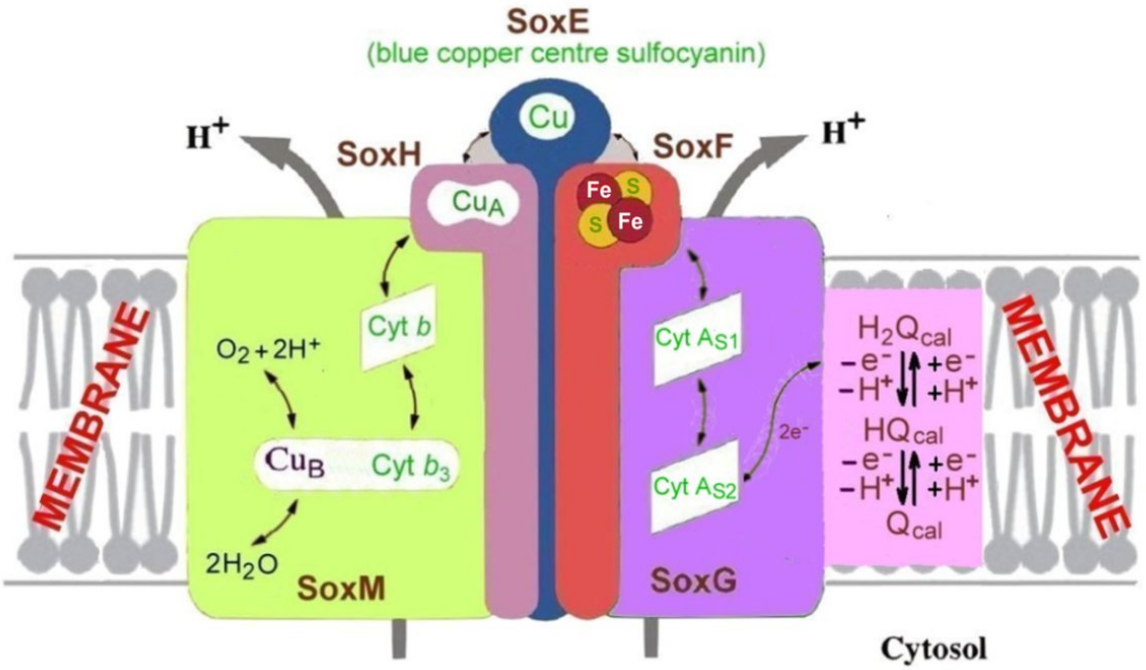

Figure 17. A representative model of the terminal oxidase supercomplex SoxM in the cell membrane of *Sulfolobus acidocaldarius*. SoxI (whose structure and function is unknown) is omitted. For a schematic structure of cytochrome A_S (also known as heme a_{587}), see [126]. The main electron transport chain of SoxM is triggered by the *Caldariella* quinoidal system through its reversible one-electron passages H_2Qcal/HQcal/Qcal (here represented as double headed arrows) that can act either as electron donor or electron acceptor depending upon the different phases of respiration. Adapted from [135].

SoxF crystallizes as a monomer and hosts a [2Fe-2S] center that constitutes the first example of a Rieske-type cluster in Archaea (Figure 18) [135].

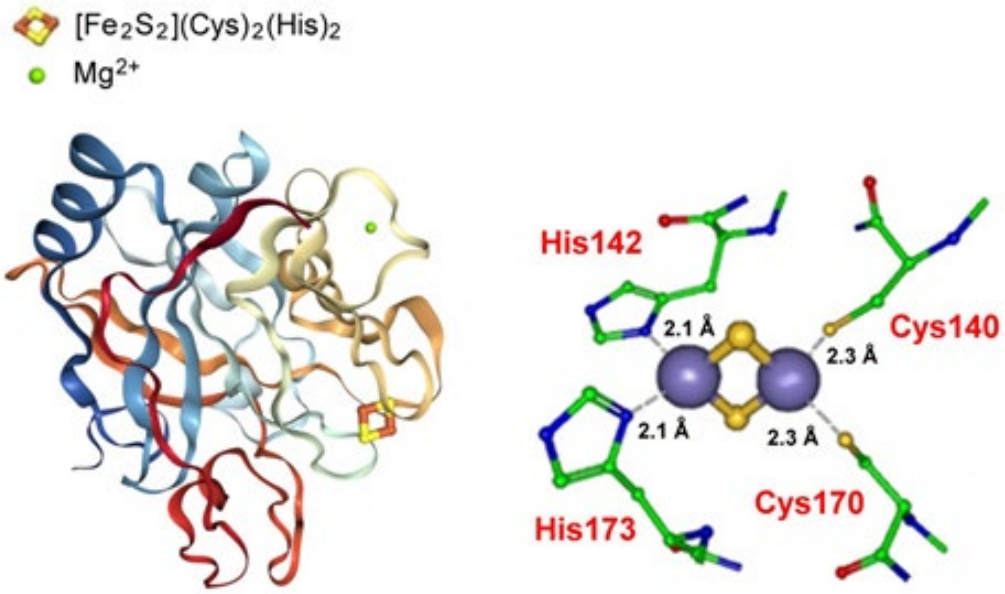

Figure 18. The molecular architecture of the component SoxF of the *Sulfolobus acidocaldarius* and the pertinent iron-sulfur protein II of SoxM oxidase. Adapted from [135]; [PDB 1JM1].

The redox properties of most components of *Sulfolobus acidocaldarius* SoxM oxidase are compiled in Table 1.

Table 1. Formal electrode potentials E°′ (V vs. NHE) for the components of *Sulfolobus acidocaldarius* SoxM oxidase.

	E°′	pH	E°′	pH	E°′	pH	Reference
$[2Fe\text{-}2S]^{2+/+}$ (SoxF)	+0.39	6.7	+0.33	7.4	+0.27	8.2	[138,139] [a]
	-	-	+0.38	7.5	-	-	[140] [e,d]
$Cu^{2+/+}$ (SoxE)	+0.30	8.0	-	-	-	-	[137] [c,f]
$Cu_A{}^{2+/+}$ (SoxH)	+0.24	6.4	-	-	-	-	[141] [f,g]
$Cu_B{}^{2+/+}$	+0.37	7.4	-	-	-	-	[142] [a]
$Fe^{3+/2+}$ (heme A_S)$_1$	+0.03	4.5	-	-	-	-	[134,135] [a]
$Fe^{3+/2+}$ (heme A_S)$_2$	+0.10	4.5	-	-	-	-	[134,135] [a]
$Fe^{3+/2+}$ (Cyt *b*)	+0.20	6.5	-	-	-	-	[134] [b]
$Fe^{3+/2+}$ (Cyt b_3)	+0.35	6.5	-	-	-	-	[134] [b]
$Q_{cal} \leftrightarrow H_2Q_{cal}$ ($\pm 2e^-$)	+0.11	6.5	-	-	-	-	[143,144] [f]

[a] Potentiometric titration monitored by EPR spectroscopy. [b] From *Sulfolobus acidocaldarius* membranes. [c] The Δ2-33 truncated form. [d] Recombinant form exploiting the Δ2-46 deletion that removes the hydrophobic domain creating a complete hydrophilic N-terminus. [e] Redox titration monitored by CD potentiometry. [f] Redox titration monitored by UV/Vis or EPR spectroscopy. [g] Recombinant form truncated to remove the short membrane anchor S6-20 in order to obtain a water-soluble gene product.

It is noted that the redox potential of the Rieske-type cluster in the pH range from 6.7 to 8.2 varies by about 80 mV/pH [138], which, being higher than 60 mV/pH for a one-proton release, suggests the existence of a second two-proton ionization that on the other hand was confirmed by EPR investigation in the pH range from 5.4 to 9.5 that at high pHs afforded a pH dependence of 120 mV/pH [139].

2.6. *Sulfurisphaera tokodaii*

The thermoacidophilic archaeon *Sulfurisphaera tokodaii* (also known as *Sulfolobus tokodaii*) was isolated from an acidic spa in Beppu Hot Springs (Kyushu, Japan) in the early 1980s. It is an obligate aerobe that grows optimally at pH 2–3 and at 75–80°C, preferably under chemoheterotrophic growth conditions [145].

There are numerous crystal structures of molecular fragments bound to *Sulfurisphaera tokodaii*, but most of them do not contain [2Fe-2S] centers. Only the glyceraldehyde oxydoreductase (GAOX) hosted by *Sulfurisphaera tokodaii* strain 7 binds [2Fe-2S] centers [146] (Figure 19).

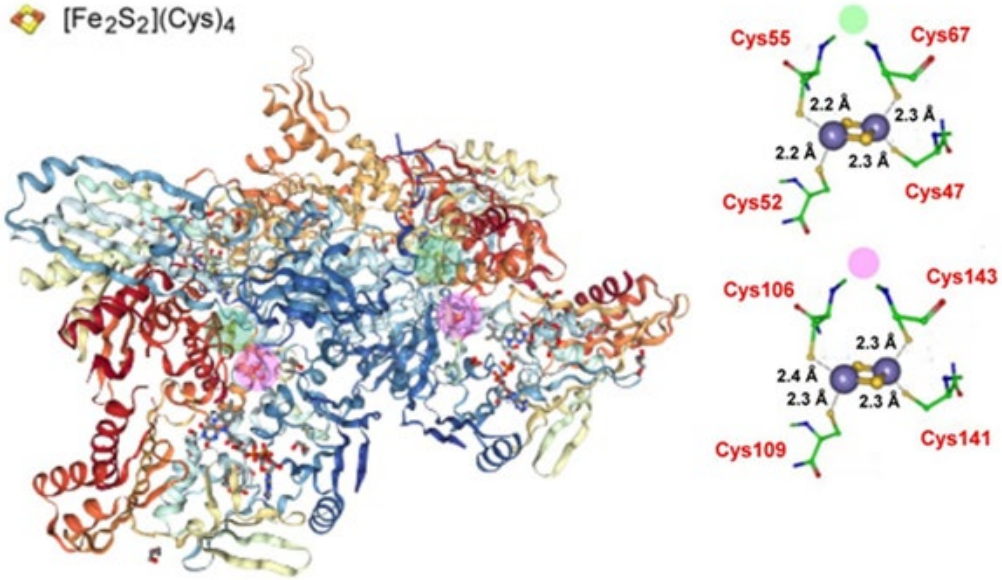

Figure 19. The overall molecular structure of the glyceraldehyde oxidoreductase (GAOR) hosted by *Sulfurisphaera tokodaii* together with the crystal structures of the two slightly different [2Fe-2S] isoforms. Adapted from [146]; [PDB 4ZOH].

The redox potentials of the two [2Fe-2S] units are not available. It must be taken into account that the activity of *Sulfurisphaera tokodaii* is part of the glycolysis process that converts glucose to pyruvate [146,147]. In reality, such a conversion can occur according to two pathways [148]: (i) the Archaeal Embden-Meyerhoff pathway; and (ii) the Archaeal Entner-Doudoroff pathway. It has been assumed that in the case of GAOX from *Sulfurisphaera tokodaii* the conversion of glucose-to-pyruvate follows the Entner-Doudoroff pathway illustrated in Figure 20 [146].

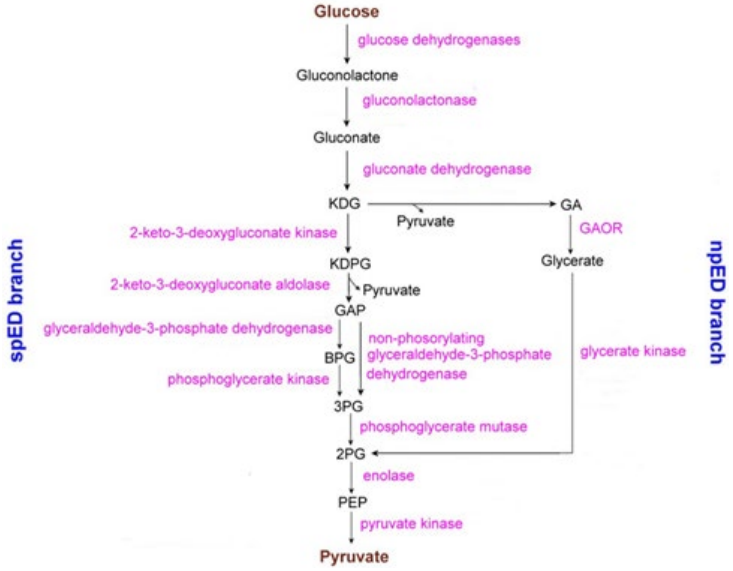

Figure 20. The Entner-Doudoroff (ED) glycolytic pathway from *Sulfurisphaera tokodaii*. spED = semiphosphorylative ED; npED = nonphosphorylative ED; KDG = 2-keto -3-deoxygluconate; GA = glyceraldehyde; KDGP = 2-keto-3-deoxy-6-phosphogluconate; GAP = glyceraldehyde-3-phosphate; BPG = 1,3 BPG = 1,3-biphosphoglycerate; 3PG = 3-phosphoglycerate; 2PG = 2-phosphoglycerate; PEP = phosphoenolpyruvate; GAOR = glyceraldehyde oxidoreductase. Adapted from [146].

The three GAOR isoenzymes, namely GAOR1, GAOR2, and GAOR3, from *Sulfurisphaera tokodaii*, have been crystallographic characterized [146]. All of them belong to the xanthine oxidoreductase superfamily and are composed of a molybdo-pyranopterin subunit (L), a flavin subunit (M), and an iron-sulfur subunit (S), forming a LMS hetero-trimer unit. In reality, the hypothesis that in Archaea the related enzyme GAPOR (i.e., glyceraldehyde-3-phosphate ferredoxin oxidoreductase) might contain a molybdopterin cofactor has been proposed [148]. Even if, at the moment, such molecular structures have not been deposited in the Protein Data Bank, Figure 21 representatively shows the molecular architecture of GAOR2 [146].

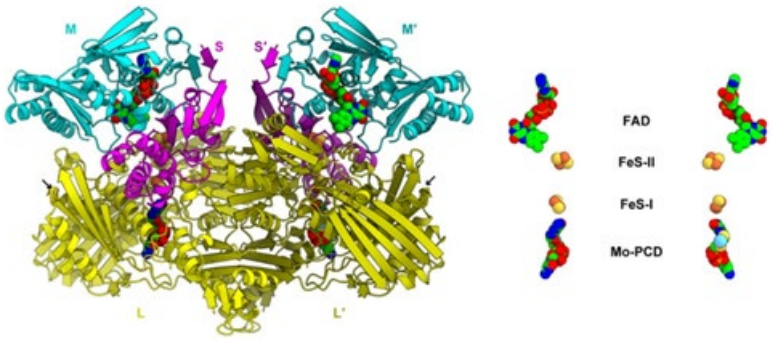

Figure 21. The overall structure of GAOR2 from *Sulfurisphaera tokodaii* together with the pertinent core cofactors. FAD = flavin adenine dinucleotide; MoPCD = Mo-pyranopterin cytosine dinucleotide. Reprinted from [146].

To our knowledge, no redox data are available for the $[2Fe\text{-}2S]^{2+/+}$ transition of *Sulfurisphaera tokodaii* glyceraldehyde oxidoreductase. In this connection, however, though it is not taken for granted that the comparison might be acceptable, we note that the glucose degradation from the molybdenum containing aldehyde oxidoreductase from *Sulfolobus acidocaldarius* (whose crystal structure is not available) hosts two [2Fe-2S] clusters, whose redox potentials are compiled in Table 2, together with those of other domains.

Table 2. Redox potentials (V, vs. NHE) of the ($[Fe_2S_2]$)$(Cys)_4$) clusters hosted by aldehyde oxidoreductases from different domains.

	$E^{\circ\prime}$ $[2Fe\text{-}2S]_I$	$E^{\circ\prime}$ $[2Fe\text{-}2S]_{II}$	pH	References
Archaea				
Sulfolobus acidocaldarius [a]	−0.30 [b]	−0.20 [b]	7.5	[149]
Bacteria				
Desulfovibrio gigas [c,d] [150,151]	−0.28 [b,e]	−0.29 [b,f]	7.6	[152]
Desulfovibrio alaskensis [g] [153]	−0.28 [b]	−0.32 [b]	9.0	[154]
Eukarya				
Mus Musculus (house mouse) [h] [155,156]	~0.0 [b,d]	~−0.1 V [b,d]	7.4	[157]

[a] The pertinent crystal structure is not known. [b] Determined by redox potentiometry monitored by EPR spectroscopy. [c] *Desulfovibrio gigas* belongs to the group of sulfate-reducing Bacteria, i.e., a member of the xanthine oxidase family, and was isolated from a sample of water from the Etang de Berre near Marseilles, France [150]. Its crystal structure is available [151]. [d] Wild-type. [e] $[2Fe\text{-}2S]_I = [Fe_2S_2](Cys)_4$ proximal to the Mo center. [f] $[2Fe\text{-}2S]_{II} = [Fe_2S_2](Cys)_4$ distal to the Mo centre. [g] A sulfate-reducing bacterium recovered from a soured oil well in Purdue Bay, Alaska [153]. [h] Its crystal structure is available [155,156].

It is evident that the archaeal iron-sulfur cluster aldehyde oxidoreductase displays a redox potential higher (more positive) than those of the other domains.

3. Conclusions and Perspectives

We discussed the known multiple enzymatic reactions triggered by Archaea. Among the pertinent subjects, we emphasized several machineries that catalyze the iron-sulfur biosynthesis (in particular the [2Fe-2S]) clusters). Moreover, we provided evidence for the eukaryotic core ISC complex machinery, the bacterial ISC machinery, the fact that one or both the bacterial ISC and SUF machineries can proceed in parallel, and the role played by the SufBC2D complex in the archaeal machinery. The pertinent molecular structures (and when available their electron-transfer capacity) were reviewed.

Nevertheless, in many of the cases dealt with while their molecular structures are available, their redox properties were investigated only in minor part. Looking ahead, we believe that either the resolution of such a lack as well as the expansion of the range of structurally and electrochemically characterized Archaea in order to enrich the knowledge of their biophysical functions would constitute significant advances.

In this connection, for example, Table 3 illustrates the electrochemical behavior of not yet structurally characterized archaeal derivatives.

Table 3. Redox potentials ($E^{\circ\prime}$ in V vs. NHE) of the $[2Fe\text{-}2S]^{2+/+}$ transition in the archaeal Rieske-type Ferredoxins (ARF).

	$E^{\circ\prime}$	pH	$E^{\circ\prime}$	pH	Reference
Sulredoxin from *Sulfololobus tokodaii* sp. (Strain 7) [a]	+0.39	5.5	+0.20	9.0	[158,159] [b]
	$E^{\circ\prime}$	pH			
Sulfolobus solfataricus (strain P-1) [c]	~−0.1	7.0			[160,161] [b]
	$E^{\circ\prime}$	pH			
Acidianus ambivalens ferredoxin 2 (RFd2) [d]	≥0.0	7.0			[162] [d]
Acidianus ambivalens subtype ferredoxin (RFd) [e]	+0.17	7.1	+0.17	7.8	[163] [f]

[a] Measured by potentiometric titration monitored by UV/vis spectroscopy. [b] Potentiometric titration. [c] Preliminarily crystallized but structurally still unresolved [161]. [d] Measured by potentiometric titration monitored by visible CD spectroscopy. [e] Structurally unresolved. [f] Measured by potentiometric titration monitored by EPR spectroscopy.

Author Contributions: M.C. and P.Z. contributed equally to this article. All authors have read and agreed to the published version of the manuscript.

Funding: This research received no external funding.

Institutional Review Board Statement: The study did not require ethical approval.

Informed Consent Statement: Not applicable.

Acknowledgments: M. Corsini acknowledges a MIUR (Ministero dell'Istruzione dell'Università e della Ricerca, Italy) grant "Dipartimento di Eccellenza 2018–2022" and P. Zanello gratefully acknowledges the University of Siena (Italy) for the access to the electronic facilities.

Conflicts of Interest: The authors declare no conflict of interest.

References

1. Kaiser, G. Classification—The Three Domain System. Community College of Baltimore Country (Cantonsville). Available online: https://bio.libretexts.org/@go/page/2699 (accessed on 3 January 2021).
2. Bar-On, Y.M.; Phillips, R.; Milo, R. The biomass distribution on Earth. *Proc. Natl. Acad. Sci. USA* **2018**, *115*, 6506–6511. [CrossRef] [PubMed]
3. Woese, C.R.; Fox, G.E. Phylogenetic structure of the prokaryotic domain: The primary kingdoms. *Proc. Natl. Acad. Sci. USA* **1977**, *74*, 5088–5090. [CrossRef] [PubMed]
4. Woese, C.R. These unusual bacteria are genealogically neither prokaryotes nor eukaryotes. This discovery means there are not two lines of descent but three: The archaebacteria, the true bacteria and the eukaryotes. *Sci. Am.* **1981**, *244*, 98–125. [CrossRef]
5. Woese, C.R. There must be a prokaryote somewhere: Microbiology's search for itself. *Microbiol. Rev.* **1994**, *58*, 1–9. [CrossRef]
6. Woese, C.R. The universal ancestor. *Proc. Natl. Acad. Sci USA* **1998**, *95*, 6854–6859. [CrossRef]
7. Woese, C.R. Interpreting the universal phylogenetic tree. *Proc. Natl. Acad. Sci. USA* **2000**, *97*, 8392–8396. [CrossRef] [PubMed]
8. Woese, C.R. On the evolution of cells. *Proc. Natl. Acad. Sci. USA* **2002**, *99*, 8742–8747. [CrossRef] [PubMed]
9. Organismal Biology. Prokaryotes: Bacteria & Archaea (See Biodiversity). Available online: https://organismalbio.biosci.gatech.edu (accessed on 26 June 2021).
10. Fabrizi de Biani, F.; Zanello, P. The competition between chemistry and biology in assembling iron-sulfur derivatives. Molecular structures and electrochemistry. Part IV. $[Fe_3S_4](SCys)_3$ proteins. *Inorg. Chim. Acta* **2017**, *455*, 319–328. [CrossRef]
11. Beinert, H. Iron-sulfur proteins: Ancient structures, still full of surprises. *J. Biol. Inorg. Chem.* **2000**, *5*, 2–15. [CrossRef]
12. Johnson, D.C.; Dean, D.; Smith, A.D.; Johnson, M.K. Structure, function, and formation of biological iron-sulfur clusters. *Annu. Rev. Biochem.* **2005**, *74*, 247–281. [CrossRef] [PubMed]
13. Lukianova, O.A.; David, S.S. A role for ironsulfur clusters in DNA repair. *Curr. Opin. Chem. Biol.* **2005**, *9*, 145–151. [CrossRef] [PubMed]
14. Fontecave, M. Iron-sulfur clusters: Ever-expanding roles. *Nat. Chem. Biol.* **2006**, *4*, 171–174. [CrossRef] [PubMed]
15. Outten, F.W. Iron-sulfur clusters as oxygen-responsive molecular switches. *Nat. Chem. Biol.* **2007**, *3*, 206–207. [CrossRef] [PubMed]
16. Wollers, S.; Layer, G.; Garcia-Serres, R.; Signor, L.; Clemancey, M.; Latour, J.-M.; Fontecave, M.; Ollagnier de Choudens, S. Iron-Sulfur (Fe-S) Cluster Assembly. *J. Biol. Chem.* **2010**, *285*, 23331–23341. [CrossRef] [PubMed]
17. Crack, J.C.; Green, J.; Thomson, A.J.; Le Brun, N.E. Iron–sulfur cluster sensor-regulators. *Curr. Opin. Chem. Biol.* **2012**, *16*, 35–44. [CrossRef]
18. Peters, J.W.; Broderick, J.B. Emerging Paradigms for Complex Iron-Sulfur Cofactor Assembly and Insertion. *Annu. Rev. Biochem.* **2012**, *81*, 429–450. [CrossRef]
19. Balk, J.; Schaedler, T.A. Iron Cofactor Assembly in Plants. *Annu. Rev. Plant Biol.* **2014**, *65*, 125–153. [CrossRef] [PubMed]
20. Sharma, S.; Sivalingam, K.; Neese, F.; Chan, G.K.-L. Low-energy spectrum of iron–sulfur clusters directly from many-particle quantum mechanics. *Nat. Chem.* **2014**, *6*, 927–933. [CrossRef] [PubMed]
21. Stiban, J.; So, M.; Kaguni, L.S. Iron-sulfur clusters in mitochondrial metabolism: Multifaceted roles of a simple cofactor. *Biochemistry* **2016**, *81*, 1066–1080. [CrossRef] [PubMed]
22. Zanello, P. The competition between chemistry and biology in assembling iron–sulfur derivatives. Molecular structures and electrochemistry. Part I. $\{Fe(S\gamma Cys)_4\}$ proteins. *Coord. Chem. Rev.* **2013**, *257*, 1777–1805. [CrossRef]
23. Zanello, P. The competition between chemistry and biology in assembling iron–sulfur derivatives. Molecular structures and electrochemistry. Part II. $\{[Fe_2S_2](S\gamma Cys)_4\}$ proteins. *Coord. Chem. Rev.* **2014**, *280*, 54–83. [CrossRef]
24. Zanello, P. The competition between chemistry and biology in assembling iron–sulfur derivatives. Molecular structures and electrochemistry. Part III. $\{[Fe_2S_2](Cys)3(X)\}$ (X = Asp, Arg, His) and $\{[Fe_2S_2](Cys)2(His)2\}$ proteins. *Coord. Chem. Rev.* **2016**, *306*, 420–442. [CrossRef]
25. Zanello, P. The competition between chemistry and biology in assembling iron–sulfur derivatives. Molecular structures and electrochemistry. Part V. $\{[Fe_4S_4](S\gamma Cys)_4\}$ proteins. *Coord. Chem. Rev.* **2017**, *335*, 172–227. [CrossRef]
26. Zanello, P.; Corsini, M. The competition between chemistry and biology in assembling iron sulfur derivatives: Molecular structures and electrochemistry. Part VI. $[Fe_4\text{-}S_4](SCys)_3$ (nonthiolate ligand) proteins. In *Reference Module in Chemistry, Molecular*

Sciences and Chemical Engineering; Elsevier: Amsterdam, The Netherlands, 2014; Available online: https://www.sciencedirect.com/science/article/pii/B9780124095472127088 (accessed on 3 January 2022).
27. Zanello, P. Structure and electrochemistry of proteins harboring iron-sulfur clusters of different nuclearities. Part I. [4Fe-4S] + [2Fe-2S] iron-sulfur proteins. *J. Struct. Biol.* **2017**, *200*, 1–19. [CrossRef] [PubMed]
28. Zanello, P. Structure and electrochemistry of proteins harboring iron-sulfur clusters of different nuclearities. Part II. [4Fe-4S] and [3Fe-4S] iron-sulfur proteins. *J. Struct. Biol.* **2018**, *202*, 250–263. [CrossRef] [PubMed]
29. Zanello, P. Structure and electrochemistry of proteins harboring iron-sulfur clusters of different nuclearities. Part III. [4Fe-4S] and [3Fe-4S] iron-sulfur proteins. *J. Struct. Biol.* **2018**, *202*, 264–274. [CrossRef] [PubMed]
30. Zanello, P. Structure and electrochemistry of proteins harboring iron-sulfur clusters of different nuclearities. Part IV. Canonical, non-canonical and hybrid iron-sulfur proteins. *J. Struct. Biol.* **2019**, *205*, 103–120. [CrossRef] [PubMed]
31. Zanello, P. Structure and electrochemistry of proteins harboring iron-sulfur clusters of different nuclearities. Part V. Nitrogenases. *Coord. Chem. Rev.* **2019**, *398*, 113004. [CrossRef]
32. Bonfio, C.; Godino, E.; Corsini, M.; de Biani, F.F.; Guella, F.G.; Mansy, S.S. Prebiotic ironsulfur peptide catalysts generate a pH gradient across model membranes of late protocells. *Nat. Catal.* **2018**, *1*, 616–623. [CrossRef]
33. Klenk, H.-P.; Clayton, R.A.; Tomb, J.-F.; White, O.; Nelson, K.E.; Ketchum, K.A.; Dodson, R.J.; Gwinn, M.; Hickey, E.K.; Peterson, J.D.; et al. The complete genome sequence of the hyperthermophilic, sulphate-reducing archaeon Archaeoglobus fulgidus. *Nature* **1997**, *390*, 591–594. [CrossRef]
34. Birkeland, N.-K.; Schönheit, P.; Poghosyan, L.; Fiebig, A.; Klenk, H.-P. Complete genome sequence analysis of *Archaeoglobus fulgidus* strain 7324 (DSM 8774), a hyperthermophilic archaeal sulfate reducer from a North Sea oil field. *Stand. Genomic Sci.* **2017**, *12*, 79. [CrossRef] [PubMed]
35. McGuirl, M.A.; Dooley, D.M. Copper-containing oxidases. *Curr. Opin. Chem. Biol.* **1999**, *3*, 138–144. [CrossRef]
36. Winterbourn, C.C. Toxicity of iron and hydrogen peroxide: The Fenton reaction. *Toxicol. Lett.* **1995**, *82/83*, 969–974. [CrossRef]
37. Prousek, Fenton chemistry in biology and medicine. *J. Pure Appl. Chem.* **2007**, *79*, 2325–2338. [CrossRef]
38. Harrison, M.D.; Jones, C.E.; Dameron, C.T. Copper chaperones: Function, structure and copper-binding properties. *J. Biol. Inorg. Chem.* **1999**, *4*, 145–153. [CrossRef] [PubMed]
39. Markossian, K.A.; Kurganov, B.I. Copper chaperones, intracellular copper trafficking proteins. Function, structure, and mechanism of action. *Biochemistry* **2003**, *68*, 827–837.
40. Pham, A.N.; Xing, G.; Miller, C.J.; Waite, T.D. Fenton-like copper redox chemistry revisited: Hydrogen peroxide and superoxide mediation of copper-catalyzed oxidant production. *J. Catal.* **2013**, *301*, 54–64. [CrossRef]
41. Kim, B.-E.; Nevitt, T.; Thiele, D.J. Mechanisms for copper acquisition, distribution and regulation. *Nat. Chem. Biol.* **2008**, *4*, 176–185. [CrossRef] [PubMed]
42. Macomber, L.; Imlay, J.A. The iron-sulfur clusters of dehydratases are primary intracellular targets of copper toxicity. *Proc. Natl. Acad. Sci. USA* **2009**, *106*, 8344–8349. [CrossRef]
43. Kühlbrandt, W. Biology, structure and mechanism of P-type ATPases. *Nat. Rev. Mol. Cell Biol.* **2004**, *5*, 282–295. [CrossRef]
44. Palmgren, M.G.; Nissen, P. P-Type ATPases. *Annu. Rev. Biophys.* **2011**, *40*, 243–266. [CrossRef]
45. Bublitz, M.; Morth, J.P.; Nissen, P. P-type ATPases at a glance. *J. Cell Sci.* **2012**, *124*, 2515–2519. [CrossRef] [PubMed]
46. Inesi, G.; Pilankatta, R.; Tadini-Buoninsegni, F. Biochemical characterization of P-type copper ATPases. *Biochem. J.* **2014**, *463*, 167–176. [CrossRef] [PubMed]
47. Palumaa, P. Copper chaperones. The concept of conformational control in the metabolism of copper. *FEBS Lett.* **2013**, *587*, 1902–1910. [CrossRef] [PubMed]
48. González-Guerrero, M.; Argüello, J.M. Mechanism of Cu+-transporting ATPases: Soluble Cu+ chaperones directly transfer Cu+ to transmembrane transport sites. *Proc. Natl. Acad. Sci. USA* **2008**, *105*, 5992–5997. [CrossRef] [PubMed]
49. Sazinsky, M.H.; LeMoine, B.; Orofino, M.; Davydov, R.; Bencze, K.Z.; Stemmler, T.L.; Hoffman, B.M.; Argüello, J.M.; Rosenzweig, A.C. Characterization and Structure of a Zn2 and [2Fe-2S]-containing Copper Chaperone from *Archaeoglobus fulgidus*. *J. Biol. Chem.* **2007**, *282*, 25950–25959. [CrossRef]
50. Boal, A.K.; Rosenzweig, A.C. Structural Biology of Copper Trafficking. *Chem. Rev.* **2009**, *109*, 4760–4779. [CrossRef]
51. Mayhew, S.G. The Redox Potential of Dithionite and SO-2 from Equilibrium Reactions with Flavodoxins, Methyl Viologen and Hydrogen plus Hydrogenase. *Eur. J. Biochem.* **1978**, *85*, 535–547. [CrossRef]
52. Melber, A.; Winge, D.R. Steps Toward Understanding Mitochondrial Fe/S Cluster Biogenesis. *Methods Enzymol.* **2018**, *599*, 265–292.
53. Frazzon, J.; Dean, D.R. Feedback regulation of iron-sulfur cluster biosynthesis. *Proc. Natl. Acad. Sci. USA* **2001**, *98*, 14751–14753. [CrossRef]
54. Mihara, H.; Esaki, N. Bacterial cysteine desulfurases: Their function and mechanisms. *Appl. Microbiol. Biotechnol.* **2002**, *60*, 12–23. [PubMed]
55. Kato, S.-I.; Mihara, H.; Kurihara, T.; Takahashi, Y.; Tokumoto, U.; Yoshimura, T.; Esaki, N. The iscS gene is essential for the biosynthesis of 2-selenouridine in tRNA and the selenocysteine-containing formate dehydrogenase H. *Proc. Natl. Acad. Sci. USA* **2002**, *99*, 5948–5952. [CrossRef] [PubMed]
56. Frazzon, J.; Fickt, J.R.; Dean, D.R. Biosynthesis of iron-sulphur clusters is a complex and highly conserved process. *Biochem. Soc. Trans.* **2002**, *30*, 680–685. [CrossRef] [PubMed]

57. Frazzon, J.; Dean, D.R. Formation of iron-sulfur clusters in bacteria: An emerging field in bioinorganic chemistry. *Curr. Opin. Chem. Biol.* **2003**, *7*, 166–173. [CrossRef]
58. Fontecave, M.; Ollagnier-de-Choudens, S. Iron-sulfur cluster biosynthesis in bacteria: Mechanisms of cluster assembly and transfer. *Arch. Biochem. Biophys.* **2008**, *474*, 226–237. [CrossRef]
59. Ali, V.; Nozak, T. Iron–Sulphur Clusters, Their Biosynthesis, and Biological Functions in Protozoan Parasites. *Adv. Parasitol.* **2013**, *83*, 1–92.
60. Roche, B.; Aussel, L.; Ezraty, B.; Mandin, P.; Py, B.; Barras, F. Iron/sulfur proteins biogenesis in prokaryotes: Formation, regulation and diversity. *Biochim. Biophys. Acta* **2013**, *1827*, 455–469. [CrossRef]
61. Kesawat, M.S.; Das, B.K.; Kumar, M.; Bhaganagare, G.R.; Manorama. An overview on Fe–S protein biogenesis from prokaryotes to eukaryotes. In *Biological Nitrogen Fixation*; de Bruijn, F.J., Ed.; John Wiley & Sons, Inc.: Hoboken, NJ, USA, 2015; Volume 1, Chapter 6; pp. 57–74.
62. Rocha, A.G.; Dancis, A. Life without Fe-S cluster. *Mol. Microbiol.* **2016**, *99*, 821–826. [CrossRef]
63. Dos Santos, P.C. *B. subtilis* as a Model for Studying the Assembly of FeS Clusters in Gram-Positive Bacteria. *Methods Enzymol.* **2017**, *595*, 185–212. [PubMed]
64. Braymer, J.J.; Lill, R. Iron sulfur cluster biogenesis and trafficking in mitochondria. *J. Biol. Chem.* **2017**, *292*, 12754–12763. [CrossRef]
65. Boniecki, M.T.; Freibert, S.A.; Mühlenhoff, U.; Lill, R.; Cygler, M. Structure and functional dynamics of the mitochondrial Fe/S cluster synthesis complex. *Nat. Commun.* **2017**, *8*, 1287. [CrossRef]
66. Di Maio, D.; Chandramouli, B.; Yan, R.; Brancato, G.; Pastore, A. Understanding the role of dynamics in the iron sulfur cluster molecular machine. *Biochim. Biophys. Acta* **2017**, *1861*, 3154–3163. [CrossRef] [PubMed]
67. Cardenas-Rodriguez, M.; Chatzi, A.; Tokatlidis, K. Iron sulfur clusters: From metals through mitochondria biogenesis to disease. *J. Biol. Inorg. Chem.* **2018**, *23*, 509–520. [CrossRef]
68. Zheng, C.; Dos Santos, P.C. Metallocluster transactions: Dynamic protein interactions guide the biosynthesis of FeS clusters in bacteria. *Biochem. Soc. Trans.* **2018**, *46*, 1593–1603. [CrossRef] [PubMed]
69. Wachnowsky, C.; Fidai, I.; Cowan, J.A. Iron-sulfur cluster biosynthesis and trafficking-impact on human disease conditions. *Metallomics* **2018**, *10*, 9–29. [CrossRef] [PubMed]
70. Pérard, J.; Ollagnier de Choudens, S. Iron-sulfur clusters biogenesis by the SUF machinery: Close to the molecular mechanism understanding. *J. Biol. Inorg. Chem.* **2018**, *23*, 581–596. [CrossRef]
71. Bai, Y.; Chen, T.; Happe, T.; Lu, Y.; Sawyer, A. Iron–sulphur cluster biogenesis via the SUF pathway. *Metallomics* **2018**, *10*, 1038–1052. [CrossRef] [PubMed]
72. Yuda, E.; Tanaka, N.; Fujishiro, T.; Yokoyama, N.; Hirabayashi, K.; Fukuyama, K.; Wada, K.; Takahashi, Y. Mapping the key residues of SufB and SufD essential for biosynthesis of iron-sulfur clusters. *Sci. Rep.* **2017**, *7*, 9387. [CrossRef]
73. Nicolet, Y.; Fontecilla-Camps, J.C. Fe-S clusters: Biogenesis and redox, catalytic, and regulatory properties. In *Bioinspired Catalysis: Metal-Sulfur Complexes*; Weigand, W., Schollhammer, P., Eds.; Wiley-VCH Verlag GmbH & Co. KGaA: Weinheim, Germany, 2015.
74. Srour, B.; Gervason, S.; Monfort, B.; D'Autréaux, B. Mechanism of Iron–Sulfur Cluster Assembly: In the Intimacy of Iron and Sulfur Encounter. *Inorganics* **2020**, *8*, 55. [CrossRef]
75. Takahashi, Y.; Nakamura, M. Functional Assignment of the ORF2-iscS-iscU-iscA-hscB-hscA-fdx-0RF3 Gene Cluster Involved in the Assembly of Fe-S Clusters. *J. Biochem.* **1999**, *126*, 917–926. [CrossRef] [PubMed]
76. Ho, T.-H.; Huynh, K.-H.; Nguyen, D.Q.; Park, H.; Jung, K.; Sur, B.; Ahn, Y.-J.; Cha, S.-S.; Kang, L.-W. Catalytic Intermediate Crystal Structures of Cysteine Desulfurase from the *Archaeon Thermococcus onnurineus* NA1. *Archaea* **2017**, *2017*, 5395293. [CrossRef] [PubMed]
77. Liu, Y.; Sieprawska-Lupa, M.; Whitman, W.B.; White, R.H. Cysteine Is Not the Sulfur Source for Iron-Sulfur Cluster and Methionine Biosynthesis in the Methanogenic Archaeon *Methanococcus maripaludis*. *J. Biol. Chem.* **2010**, *285*, 31923–31949. [CrossRef]
78. Boyd, E.S.; Thomas, K.M.; Dai, Y.; Boyd, J.M.; Outten, F.W. Interplay between Oxygen and Fe-S Cluster Biogenesis: Insights from the Suf Pathway. *Biochemistry* **2014**, *53*, 5834–5847. [CrossRef]
79. Boyd, J.M.; Drevland, R.M.; Downs, D.M.; Graham, D.E. Archaeal ApbC/Nbp35 Homologs Function as Iron-Sulfur Cluster Carrier Proteins. *J. Bacteriol.* **2009**, *191*, 1490–1497. [CrossRef]
80. Garcia, P.S.; Gribaldo, S.; Py, B.; Barras, F. The SUF system: An ABC ATPase-dependent protein complex with a role in Fe-S cluster biogenesis. *Res. Microbiol.* **2019**, *170*, 426–434. [CrossRef]
81. Liu, Y.; Beer, L.L.; Whitman, W.B. Sulfur metabolism in archaea reveals novel processes. *Environ. Microbiol.* **2012**, *14*, 2632–2644. [CrossRef] [PubMed]
82. Boyd, J.M.; Pierik, A.J.; Netz, D.J.A.; Lill, R.; Downs, D.M. Bacterial {ApbC} Can Bind and Effectively Transfer Iron-Sulfur Clusters. *Biochemistry* **2008**, *47*, 8195–8202. [CrossRef] [PubMed]
83. Boyd, J.M.; Sondelski, J.L.; Downs, D.M. Bacterial ApbC Protein Has Two Biochemical Activities That Are Required for in Vivo Function. *J. Biol. Chem.* **2009**, *284*, 110–118. [CrossRef]
84. Marinoni, E.N.; de Oliveira, J.S.; Nicolet, Y.; Raulfs, E.C.; Amara, P.; Dean, D.R.; Fontecilla-Camps, J.C. (IscS-IscU)2 Complex Structures Provide Insights into Fe2S2 Biogenesis and Transfer. *Angew. Chem. Int. Ed.* **2012**, *51*, 5439–5442. [CrossRef] [PubMed]

85. Raulfs, E.C.; O'Carroll, I.P.; Dos Santos, P.C.; Unciuleac, M.-C.; Dean, D.R. In vivo iron-sulfur cluster formation. *Proc. Natl. Acad. Sci. USA* **2008**, *105*, 8591–8596. [CrossRef]
86. Yamanaka, Y.; Zeppieri, L.; Nicolet, Y.; Marinoni, E.N.; de Oliveira, J.S.; Odaka, M.; Dean, D.R.; Fontecilla-Camps, J.C. Crystal structure and functional studies of an unusuall-cysteine desulfurase from Archaeoglobus fulgidus. *Dalton Trans.* **2013**, *42*, 3092–3099. [CrossRef] [PubMed]
87. Pagnier, A.; Nicolet, Y.; Fontecilla-Camps, J.C. IscS from *Archaeoglobus fulgidus* has no desulfurase activity but may provide a cysteine ligand for [Fe2S2] cluster assembly. *Biochim. Biophys. Acta* **2015**, *1853*, 1457–1463. [CrossRef] [PubMed]
88. Nývltová, E.; Suták, R.; Harant, K.; Sedinová, M.; Hrdý Jan Pačes, I.; Vlčk, Č.; Tachezy, J. NIF-type iron-sulfur cluster assembly system is duplicated and distributed in the mitochondria and cytosol of *Mastigamoeba balamuthi*. *Proc. Natl. Acad. Sci. USA* **2013**, *110*, 7371–7376. [CrossRef]
89. Bell, S.D.; Jackson, S.P. Mechanism and regulation of transcription in archaea. *Curr. Opin. Microbiol.* **2001**, *4*, 208–213. [CrossRef]
90. Brochier, C.; Forterre, P.; Gribaldo, S. An emerging phylogenetic core of Archaea: Phylogenies of transcription and translation machineries converge following addition of new genome sequences. *BMC Evol. Biol.* **2005**, *5*, 36. [CrossRef] [PubMed]
91. Barry, E.R.; Bell, S.D. DNA Replication in the Archaea. *Microbiol. Mol. Biol. Rev.* **2006**, *70*, 876–887. [CrossRef]
92. Greci, M.D.; Bell, S.D. Archaeal DNA Replication. *Annu. Rev. Microbiol.* **2020**, *74*, 65–80. [CrossRef]
93. Lindås, A.C.; Karlsson, E.A.; Lindgren, M.T.; Ettema, T.J.G.; Bernander, R. A unique cell division machinery in the Archaea. *Proc. Natl. Acad. Sci. USA* **2008**, *1051*, 18942–18946. [CrossRef]
94. Iwasaki, T. Iron-Sulfur World in Aerobic and Hyperthermoacidophilic Archaea Sulfolobus. *Archaea* **2010**, *2010*, 842639. [CrossRef]
95. O'Donnell, M.; Langston, L.; Stillman, B. Principles and concepts of DNA replication in bacteria, archaea, and bacteria. *Cold Spring Harb. Perspect. Biol.* **2013**, *5*, a010108.
96. Han, W.; Shen, Y.; She, Q. Nanobiomotors of archaeal DNA repair machineries: Current research status and application potential. *Cell Biosci.* **2014**, *4*, 32. [CrossRef] [PubMed]
97. Phung, D.K.; Etienne, C.; Batista, M.; Langendiik-Genevaux, P.; Moalic, Y.; Laurent, S.; Liu, S.; Morales, V.; Jebbar, M.; Fichant, G.; et al. RNA processing machineries in Archaea: The 5′-3′ exoribonuclease aRNase J of the β-CASP family is engaged specifically with the helicase ASH-Ski2 and the 3′-5′ exoribonucleolytic RNA exosome machinery. *Nucleic Acid Res.* **2020**, *48*, 3832–3847. [CrossRef] [PubMed]
98. Lill, R.; Freibert, S.-A. Mechanisms of Mitochondrial Iron-Sulfur Protein Biogenesis. *Annu. Rev. Biochem.* **2020**, *89*, 471–499. [CrossRef] [PubMed]
99. Weiler, B.D.; Brück, M.-C.; Kothe, I.; Bill, E.; Lill, R.; Mühlenhoff, U. Mitochondrial [4Fe-4S] protein assembly involves reductive [2Fe-2S] cluster fusion on ISCA1-ISCA2 by electron flow from ferredoxin FDX2. *Proc. Natl. Acad. Sci. USA* **2020**, *117*, 20555–20565. [CrossRef] [PubMed]
100. Lill, R. Function and biogenesis of iron-sulphur proteins. *Nature* **2009**, *460*, 831–838. [CrossRef]
101. Nozhevnikova, A.N.; Chudina, V.I. Morphology of the thermophilic acetate bacterium *Methanothrix thermoacetophila*. *Mikrobiologiia* **1984**, *53*, 756–760.
102. Boone, D.R.; Kamagata, Y.J. Rejection of the species *Methanothrix soehngenii* ^{VP} and the genus *Methanothrix* ^{VP} as *nomina confusa*, and transfer of *Methanothrix thermophila* ^{VP} to the genus *Methanosaeta* ^{VP} as *Methanosaeta thermophila* comb. nov. Request for an Opinion. *Syst. Bacteriol.* **1998**, *48*, 1079–1080. [CrossRef]
103. *Methanothrix thermoacetophila* PT strain: PT. Available online: https://www.ncbi.nlm.nih.gov/bioproject/?term=PRJNA15765 (accessed on 3 January 2022).
104. *Methanothrix thermoacetophila* (strain DSM 6194/JCM 14653/NBRC 101360/PT) (*Methanothrix thermoacetophila*). Available online: https://www.uniprot.org/proteomes/UP000000674 (accessed on 3 January 2022).
105. Kunichika, K.; Nakamura, R.; Fujishiro, T.; Takahashi, Y. The Structure of the Dimeric State of IscU Harboring Two Adjacent [2Fe-2S] Clusters Provides Mechanistic Insights into Cluster Conversion to [4Fe-4S]. *Biochemistry* **2021**, *60*, 1569–1572. [CrossRef] [PubMed]
106. Kunichika, K.; Fujishiro, T.; Takahashi, Y. Crystal Structure of IscU H106C Variant. Available online: https://www.rcsb.org/structure/7CNV (accessed on 3 January 2022).
107. Amo, T.; Luz, M.; Paje, F.; Inagaki, A.; Ezaki, S.; Atomi, H.; Imanaka, T. *Pyrobaculum calidifontissp*. nov., a novel hyperthermophilic archaeon that grows in atmospheric air. *Archaea* **2002**, *1*, 113–121. [CrossRef]
108. Lemak, S. Structural and Biochemical Characterization of CRISPR-Associated Cas4 Nucleases from a Prokaryotic Defense System. Master's Thesis, Department of Chemical Engineering and Applied Chemistry, University of Toronto, Toronto, ON, Canada, 2013; p. 866.
109. Zhang, J.; Kasciukovic, T.; White, M.F. The CRISPR Associated Protein Cas4 Is a 5′ to 3′ DNA Exonuclease with an Iron-Sulfur Cluster. *PLoS ONE* **2012**, *7*, e47232. [CrossRef] [PubMed]
110. Shmakova, S.A.; Makarova, K.S.; Wolf, Y.I.; Severinova, K.V.; Koonin, E.V. Systematic prediction of genes functionally linked to CRISPR-Cas systems by gene neighborhood analysis. *Proc. Natl. Acad. Sci. USA* **2018**, *115*, E5307–E5316. [CrossRef] [PubMed]
111. Makarov, K.S.; Wolf, Y.I.; Koonin, E.V. Classification and Nomenclature of CRISPR-Cas Systems: Where from Here? *CRISPR J.* **2018**, *1*, 325–336. [CrossRef] [PubMed]
112. Koonin, E.V.; Makarova, K.S. Origins and evolution of CRISPR-Cas systems. *Philos. Trans. R. Soc. Lond. B Biol. Sci.* **2019**, *374*, 20180087. [CrossRef] [PubMed]

113. Makarova, K.S.; Wolf, Y.I.; Alkhnbashi, O.S.; Costa, F.; Shah, S.A.; Saunders, S.J.; Barrangou, R.; Brouns, S.J.J.; Charpentier, E.; Haft, D.H.; et al. An updated evolutionary classification of CRISPR-Cas systems. *Nat. Rev. Microbiol.* **2015**, *13*, 722–736. [CrossRef]
114. Burstein, D.; Harrington, L.B.; Strutt, S.C.; Probst, A.J.; Anantharaman, K.; Thomas, B.C.; Doudna, J.A.; Banfield, J.F. New CRISPR-Cas systems from uncultivated microbes. *Nature* **2017**, *542*, 237–241. [CrossRef]
115. Lemak, S.; Nocek, B.; Beloglazova, N.; Skarina, T.; Flick, R.; Brown, G.; Joachimiak, A.; Savchenko, A.; Yakunin, A.F. The CRISPR-associated Cas4 protein Pcal_0546 from *Pyrobaculum calidifontis* contains a [2Fe-2S] cluster: Crystal structure and nuclease activity. *Nucleic Acids Res.* **2014**, *42*, 11144–11155. [CrossRef]
116. Lin, J.; Zhang, L.; Lai, S.; Ye, K. Structure and Molecular Evolution of CDGSH Iron-Sulfur Domains. *PLoS ONE* **2011**, *6*, e24790. [CrossRef]
117. Sengupta, S.; Nechushtai, R.; Jennings, P.A.; Onuchic, J.N.; Padilla, P.A.; Azad, R.K.; Mittler, R. Phylogenetic analysis of the CDGSH iron-sulfur binding domain reveals its ancient origin. *Sci. Rep.* **2018**, *8*, 4840. [CrossRef]
118. González, J.M.; Masuchi, Y.; Robb, F.T.; Ammerman, J.W.; Maeder, D.L.; Yanagibayashi, M.; Tamaoka, J.; Kato, C. *Pyrococcus horikoshii* sp. nov., a hyperthermophilic archaeon isolated from a hydrothermal vent at the Okinawa Trough. *Extremophiles* **1998**, *2*, 123–130. [CrossRef] [PubMed]
119. Kawarbayasi, Y.; Sawada, M.; Horikawa, H.; Haikawa, Y.; Hino, Y.; Yamamoto, S.; Sekine, M.; Baba, S.-I.; Kosugi, H.; Hosoyama, A.; et al. Complete Sequence and Gene Organization of the Genome of a Hyper-thermophilic Archaebacterium, Pyrococcus horikoshii OT3 (Supplement). *DNA Res.* **1998**, *5*, 147–155. [CrossRef]
120. Shigi, N. Recent Advances in Our Understanding of the Biosynthesis of Sulfur Modifications in tRNAs. *Front. Microbiol.* **2018**, *9*, 2679. [CrossRef] [PubMed]
121. ttuA-tRNA-5-methyluridine(54) 2-sulfurtransferase—Pyrococcus horikoshii (Strain ATCC 700860/DSM 12428/JCM 9974/NBRC 100139/OT-3)—ttuA Gene & Protein. Available online: https://www.uniprot.org/uniprot/O58038 (accessed on 26 June 2021).
122. Arragain, S.; Bimai, O.; Legrand, P.; Caillat, S.; Ravanat, J.-L.; Touati, N.; Binet, L.; Atta, M.; Fontecave, M. Nonredox thiolation in tRNA occurring via sulfur activation by a [4Fe-4S] cluster. *Proc. Natl. Acad. Sci. USA* **2017**, *114*, 7355–7360. [CrossRef] [PubMed]
123. Darland, G.; Brock, T.D. *Bacillus acidocaldarius* sp. nov., an Acidophilic Thermophilic Spore-forming Bacterium. *Gen. J. Microbiol.* **1971**, *67*, 9–15. [CrossRef]
124. Brock, T.D.; Brock, K.M.; Belli, R.T.; Weiss, R.L. Sulfolobus: A new genus of sulfur-oxidizing bacteria living at low pH and high temperature. *Arch. Microbiol.* **1972**, *84*, 54–68. [CrossRef]
125. Moll, R.; Schäfer, G. Chemiosmotic H+ cycling across the plasma membrane of the thermoacidophilic archaebacterium *Sulfolobus acidocaldarius*. *FEBS Lett.* **1988**, *232*, 359–363. [CrossRef]
126. Lübben, M.; Schäfer, G. Chemiosmotic energy conversion of the archaebacterial thermoacidophile *Sulfolobus acidocaldarius*: Oxidative phosphorylation and the presence of an F0-related N,N′-dicyclohexylcarbodiimide-binding proteolipid. *J. Bacteriol.* **1989**, *171*, 6106–6116. [CrossRef] [PubMed]
127. Anemüller, S.; Lübben, M.; Schäfer, G. The respiratory system of *Sulfolobus acidocaldarius*, a thermoacidophilic archaebacterium. *FEBS Lett.* **1985**, *193*, 83–87. [CrossRef]
128. Castresana, J.; Lübben, M.; Saraste, M.J. New Archaebacterial Genes Coding for Redox Proteins: Implications for the Evolution of Aerobic Metabolism. *Mol. Biol.* **1995**, *250*, 202–210. [CrossRef] [PubMed]
129. Gleißner, M.; Kaiser, U.; Antonopoulos, E.; Schäfer, G. The Archaeal SoxABCD Complex Is a Proton Pump in *Sulfolobus acidocaldarius*. *J. Biol. Chem.* **1997**, *272*, 8417–8426. [CrossRef]
130. Lübben, M.; Warne, A.; Albracht, S.P.J.; Saraste, M. The purified SoxABCD quinol oxidase complex of *Sulfolobus acidocaldarius* contains a novel haem. *Mol. Microbiol.* **1994**, *13*, 327–335. [CrossRef] [PubMed]
131. Lübben, M.; Morand, K. Novel prenylated hemes as cofactors of cytochrome oxidases. Archaea have modified hemes A and O. *J. Biol. Chem.* **1994**, *269*, 21473–21479. [CrossRef]
132. Schäfer, G.; Pursckhe, W.; Schmidt, C.L. On the origin of respiration: Electron transport proteins from archaea to man. *FEMS Microbiol. Rev.* **1996**, *18*, 173–188. [CrossRef]
133. Lappalainnen, P.; Sarraste, M. The binuclear CuA centre of cytochrome oxidase. *Biochim. Biophys. Acta* **1994**, *1187*, 222–225. [CrossRef]
134. Komorowski, L.; Verheyen, W.; Schäfer, G. The Archaeal Respiratory Supercomplex SoxM from *S. acidocaldarius* Combines Features of Quinole and Cytochrome c Oxidases. *Biol. Chem.* **2002**, *383*, 1791–1799. [CrossRef] [PubMed]
135. Bönisch, H.; Schmidt, C.L.; Schäfer, G.; Ladenstein, R. The Structure of the Soluble Domain of an Archaeal Rieske Iron-Sulfur Protein at 1.1 Å Resolution. *J. Mol. Biol.* **2002**, *319*, 791–805. [CrossRef]
136. Schäfer, G.; Engelhard, M.; Müller, V. Bioenergetics of the Archaea. *Microbiol. Mol. Biol. Rev.* **1999**, *63*, 570–620. [CrossRef] [PubMed]
137. Komorowski, L.; Schäfer, G. Sulfocyanin and subunit II, two copper proteins with novel features, provide new insight into the archaeal SoxM oxidase supercomplex. *FEBS Lett.* **2001**, *487*, 351–355. [CrossRef]
138. Anemüller, S.; Schmidt, C.L.; Schäfer, G.; Teixeira, M. Evidence for a Rieske-type FeS center in the thermoacidophilic archaebacterium *Sulfolobus acidocaldarius*. *FEBS Lett.* **1993**, *318*, 61–64. [CrossRef]
139. Anemüller, S.; Schmidt, C.L.; Schäfer, G.; Bill, E.; Trautwein, A.X.; Teixeira, M. Evidence for a Two-Proton-Dependent Redox Equilibrium in an Archaeal Rieske Iron-Sulfur Cluster. *Biochem. Biophys Res. Commun.* **1994**, *202*, 252–257. [CrossRef] [PubMed]

140. Schmidt, C.L.; Hatzfeld, O.M.; Petersen, A.; Link, T.; Schäfer, G. Expression of the *Solfolobus acidocaldarius* Rieske Iron Sulfur Protein II (SOXF) with the Correctly Inserted [2Fe-2S] Cluster in *Escherichia coli*. *Biochem. Biophys Res. Commun.* **1997**, *234*, 283–287. [CrossRef] [PubMed]
141. Komorowski, L.; Anemüller, S.; Schäfer, G. Expression and Characterization of a Recombinant CuA-Containing Subunit II from an Archaeal Terminal Oxidase Complex. *J. Bioenerg. Biomembr.* **2001**, *33*, 27–34. [CrossRef] [PubMed]
142. Anemüller, S.; Bill, E.; Schäfer, G.; Trautwein, A.X.; Teixeira, M. EPR studies of cytochrome aa3 from *Sulfolobus acidocaldarius*. Evidence for a binuclear center in archaebacterial terminal oxidase. *Eur. J. Biochem.* **1992**, *210*, 133–138. [CrossRef] [PubMed]
143. Schäfer, G.; Anemüller, S.; Moll, R.; Gleissner, M.; Schmidt, C.L. Has Sulfolobus an Archaic Respiratory System? Structure, Function and Genes of its Components. *System. Appl. Microbiol.* **1993**, *16*, 544–555. [CrossRef]
144. Schäfer, G.; Moll, R.; Schmidt, C.L. Respiratory enzymes from *Sulfolabus acidocaldarius*. *Methods Enzymol.* **2001**, *331*, 369–410.
145. Suzuki, T.; Iwasaki, T.; Uzawa, T.; Hara, K.; Nemoto, N.; Kon, T.; Ueki, T.; Yamagishi, A.; Oshima, T. *Sulfolobus tokodaii* sp. nov. (f. *Sulfolobus* sp. strain 7), a new member of the genus *Sulfolobus* isolated from Beppu Hot Springs, Japan. *Extremophiles* **2002**, *6*, 39–44. [CrossRef] [PubMed]
146. Wakagi, T.; Nishimasu, H.; Miyake, M.; Fushinobu, S. Archaeal Mo-Containing Glyceraldehyde Oxidoreductase Isozymes Exhibit Diverse Substrate Specificities through Unique Subunit Assemblies. S. *PLoS ONE* **2016**, *11*, e0147333. [CrossRef] [PubMed]
147. Bräsen, C.; Esser, D.; Rauch, B.; Siebers, B. Carbohydrate Metabolism in Archaea: Current Insights into Unusual Enzymes and Pathways and Their Regulation. *Microbiol. Mol. Biol. Rev.* **2014**, *78*, 89–175. [CrossRef] [PubMed]
148. Sato, T.; Atomi, H. Novel metabolic pathways in Archaea. *Curr. Opin. Microbiol.* **2011**, *14*, 307–314. [CrossRef] [PubMed]
149. Kardinahl, S.; Schmidt, C.L.; Hansen, T.; Anemüller, S.; Petersen, A.; Schäfer, G. The strict molybdate-dependence of glucose-degradation by the thermoacidophile *Sulfolobus acidocaldariusreveals* the first crenarchaeotic molybdenum containing enzyme—An aldehyde oxidoreductase. *Eur. J. Biochem.* **1999**, *260*, 540–548. [CrossRef]
150. Le Gall, J. A new species of desulfovibrio. *J. Bacteriol.* **1963**, *86*, 1120. [CrossRef]
151. Rebelo, J.M.; Dias, J.M.; Huber, R.; Moura, J.J.G.; Romão, M.J. Structure refinement of the aldehyde oxidoreductase from *Desulfovibrio gigas* (MOP) at 1.28 Å. *J. Biol. Inorg. Chem.* **2001**, *6*, 791–800. [CrossRef] [PubMed]
152. Correia dos Santos, M.M.; Sousa, P.M.P.; Gonçalves, M.L.S.; Romão, M.J.; Moura, I.; Moura, J.J.G. Direct electrochemistry of the Desulfovibrio gigas aldehyde oxidoreductase. *Eur. J. Biochem.* **2004**, *271*, 1329–1338. [CrossRef] [PubMed]
153. Feio, M.J.; Zinkevich, V.; Beech, I.B.; Llobet-Brossa, E.; Eaton, P.; Schmitt, J.; Guezennec, J. *Desulfovibrio alaskensis* sp. nov., a sulphate-reducing bacterium from a soured oil reservoir. *Int. J. Syst. Evol. Microbiol.* **2004**, *54*, 1747–1752. [CrossRef] [PubMed]
154. Andrade, S.L.A.; Brondino, C.D.; Feio, M.J.; Moura, I.; Moura, J.J.G. Aldehyde oxidoreductase activity in *Desulfovibrio alaskensis* NCIMB 13491. *Eur. J. Biochem.* **2000**, *267*, 2054–2061. [CrossRef]
155. Romão, M.J.; Coelho, C.; Santos-Silva, T.; Foti, A.; Terao, M.; Garattini, E.; Leimkühler, S. Structural basis for the role of mammalian aldehyde oxidases in the metabolism of drugs and xenobiotics. *Curr. Opin. Chem. Biol.* **2017**, *37*, 39–47. [CrossRef]
156. Coelho, C.; Mahro, M.; Trincão, J.; Carvalho, A.T.P.; Ramos, M.J.; Terao, M.; Garattini, E.; Leimkühler, S.; Romão, M.J. The First Mammalian Aldehyde Oxidase Crystal Structure. *J. Biol. Chem.* **2012**, *287*, 40690–40702. [CrossRef]
157. Mahro, M.; Brás, N.F.; Cerqueira, N.M.F.S.A.; Teutloff, C.; Coelho, C.; Romão, M.J.; Leimkühler, S. Identification of Crucial Amino Acids in Mouse Aldehyde Oxidase 3 That Determine Substrate Specificity. *PLoS ONE* **2013**, *8*, e82285. [CrossRef]
158. Iwasaki, T.; Imaii, T.; Urushiyama, A.; Oshima, T. Redox-linked Ionization of Sulredoxin, an Archaeal Rieske-type [2Fe-2S] Protein from *Sulfolobus* sp. Strain 7. *J. Biol. Chem.* **1996**, *271*, 27659–27663. [CrossRef] [PubMed]
159. Iwasaki, T.; Kounosu, A.; Dikanov, S.A. The [2Fe-2S] cluster in sulredoxin from the thermoacidophilic *Sulfolobus tokodaii* strain 7, a novel water-soluble Rieske-type protein. In *EPR in the 21st Century*; Kawamori, A., Yamauchi, J., Ohta, H., Eds.; Elsevier Science: Amsterdam, The Netherlands, 2002; pp. 488–493.
160. Kounosu, A.; Li, Z.; Cosper, N.J.; Shokes, J.E.; Scott, R.A.; Imai, T.; Urushiyama, A.; Iwasaki, T. Engineering a Three-cysteine, One-histidine Ligand Environment into a New Hyperthermophilic Archaeal Rieske-type [2Fe-2S] Ferredoxin from *Sulfolobus solfataricus*. *J. Biol. Chem.* **2004**, *279*, 12519–12528. [CrossRef]
161. Bandeiras, T.M.; Freitas, M.C.; Petrasch, D.; Kletzin, A.; Frazão, C. SAD phasing towards structure determination of a thermostable Rieske ferredoxin with a novel stabilizing disulfide bridge. *Acta Cryst.* **2013**, *F69*, 555–558. [CrossRef]
162. Botelho, H.M.; Leal, S.S.; Veith, A.; Prosinecki, V.; Bauer, C.; Froöhlich, R.; Kletzin, A.; Gomes, C.M. Role of a novel disulfide bridge within the all-beta fold of soluble Rieske proteins. *J. Biol. Inorg. Chem.* **2010**, *15*, 271–281. [CrossRef] [PubMed]
163. Kletzin, A.; Ferreira, A.S.; Hechler, T.; Bandeiras, T.M.; Teixeira, M.; Gomes, C.M. A Rieske ferredoxin typifying a subtype within Rieske proteins: Spectroscopic, biochemical and stability studies. *FEBS Lett.* **2005**, *579*, 1020–1026. [CrossRef] [PubMed]